

Supporting information: The importance of relativistic effects for platinum complexes with light-activated activity against cancer cells.

ASSIGNMENT OF ELECTRONIC TRANSITIONS

4c			
Energy nm (eV)	Osc. str- ($\times 10^{-4}$)	Orbitals (weight)	Interval
217.2 (5.71)	92.0	$\pi(4) \rightarrow 82$ 0.31 $\pi(3) \rightarrow 87$ 0.28 $\pi(4) \rightarrow 84$ 0.27	6
270.3 (4.59)	135	$p(2) \rightarrow d(4)$ 0.42 $p(2) \rightarrow d(3)$ 0.39 $p(1) \rightarrow d(4)$ 0.24	5
260.2 (4.77)	119	$p(2) \rightarrow d(3)$ 0.52 $\pi(3) \rightarrow d(4)$ 0.32 $p(1) \rightarrow d(3)$ 0.25	
250.3 (4.95)	240	$\pi(2) \rightarrow d(4)$ 0.54 $p(1) \rightarrow d(3)$ 0.29 $p(2) \rightarrow d(4)$ 0.20	
249.0 (4.98)	102	$\pi(2) \rightarrow d(4)$ 0.53 $p(2) \rightarrow d(4)$ 0.30 $\pi(3) \rightarrow d(4)$ 0.20	
245.0 (5.06)	138	$p(1) \rightarrow d(3)$ 0.46 $\pi(3) \rightarrow d(4)$ 0.40 $\pi(2) \rightarrow d(4)$ 0.26	
274.8 (4.51)	3145	$\pi(2) \rightarrow d(3)$ 0.62 $p(2) \rightarrow d(3)$ 0.14 $\pi(2) \rightarrow d(4)$ 0.12	4
292.7 (4.24)	0.00	$d/p \rightarrow d(3)$ 0.45 $\pi(1) \rightarrow d(3)$ 0.34 $\pi(4) \rightarrow 87$ 0.13	3
286.5 (4.33)	0.00	$d/p \rightarrow d(3)$ 0.53 $\pi(4) \rightarrow 87$ 0.16 $\pi(4) \rightarrow 86$ 0.14	
275.8 (4.50)	9.00	$d/p \rightarrow d(3)$ 0.38 $\pi(1) \rightarrow d(3)$ 0.30 $\pi(1) \rightarrow d(4)$ 0.23	
358.9 (3.46)	17.0	$\pi(3) \rightarrow d(3)$ 0.65 $\pi(2) \rightarrow d(3)$ 0.13 $\pi(4) \rightarrow 85$ 0.12	2
324.2 (3.82)	0.00	$\pi(3) \rightarrow 86$ 0.42 $\pi(4) \rightarrow 84$ 0.32 $\pi(4) \rightarrow 85$ 0.25	
308.1 (4.02)	5.00	$p(1) \rightarrow d(4)$ 0.45 $\pi(3) \rightarrow d(4)$ 0.38 $p(2) \rightarrow d(4)$ 0.23	
308.0 (4.03)	2.00	$p(1) \rightarrow d(4)$ 0.45 $\pi(3) \rightarrow d(4)$ 0.37 $p(2) \rightarrow d(4)$ 0.23	
307.8 (4.03)	0.00	$p(1) \rightarrow d(4)$ 0.46 $\pi(3) \rightarrow d(4)$ 0.37 $p(2) \rightarrow d(4)$ 0.23	
450.9 (2.75)	0.00	$\pi(4) \rightarrow d(3)$ 0.65 $p(3) \rightarrow d(3)$ 0.19 $d/p \rightarrow d(3)$ 0.09	1
425.4 (2.91)	0.00	$\pi(2) \rightarrow d(3)$ 0.66 $\pi(3) \rightarrow d(3)$ 0.14 $\pi(1) \rightarrow 85$ 0.09	
411.4 (3.01)	0.00	$p(3) \rightarrow d(4)$ 0.54 $p(3) \rightarrow d(3)$ 0.28 $\pi(4) \rightarrow d(4)$ 0.27	
406.1 (3.05)	2.00	$\pi(3) \rightarrow d(3)$ 0.63 $\pi(4) \rightarrow 85$ 0.15 $\pi(2) \rightarrow d(3)$ 0.13	
402.0 (3.08)	0.00	$p(3) \rightarrow d(3)$ 0.61 $p(3) \rightarrow d(4)$ 0.24 $p(3) \rightarrow 87$ 0.12	

TABLE S1: Transitions and assignments for the *trans*-Pt complex, calculated with 4c-CAM-B3LYP. In each region (labels **1–6**), the five most intense transitions were selected.

NR				
Energy nm (eV)	Osc. str.($\times 10^{-4}$)	Orbitals (weight)	Interval	
296.6 (4.18)	343	p(2) \rightarrow d(2) 0.53	5	
		π (2) \rightarrow d(3) 0.28		
		π (2) \rightarrow d(3) 0.25		
289.4 (4.28)	253	π (3) \rightarrow d(3) 0.41		
		p(1) \rightarrow d(2) 0.39		
		p(2) \rightarrow d(2) 0.27		
280.7 (4.42)	1423	p(1) \rightarrow d(2) 0.50		
		π (3) \rightarrow d(3) 0.35		
		π (3) \rightarrow d(2) 0.22		
277.7 (4.46)	32.0	π (1) \rightarrow d(2) 0.51		
		d/p \rightarrow d(2) 0.33		
		d(1) \rightarrow d(2) 0.25		
277.3 (4.47)	737	π (2) \rightarrow d(3) 0.58		
		p(1) \rightarrow d(3) 0.21		
		p(2) \rightarrow d(2) 0.20		
303.1 (4.09)	2383	π (3) \rightarrow d(2) 0.43	4	
		π (2) \rightarrow d(2) 0.33		
		π (3) \rightarrow d(3) 0.30		
403.8 (3.07)	13.0	π (2) \rightarrow d(2) 0.54	2	
		π (3) \rightarrow d(2) 0.43		
		π (4) \rightarrow 85 0.08		

TABLE S2: Transitions and assignments for the *trans*-Pt complex, calculated with NR-CAM-B3LYP. In each region (labels **2–5**), the five most intense transitions were selected.

SR			
Energy nm (eV)	Osc. str. ($\times 10^{-4}$)	Orbitals (weight)	Interval
217.2 (5.71)	0.0	$\pi(3) \rightarrow \pi(5)$ 0.33	6
		$d/p(1) \rightarrow d(4)$ 0.27	
		$\pi(2) \rightarrow 84$ 0.27	
217.0 (5.71)	94.0	$\pi(3) \rightarrow 82$ 0.33	
		$\pi(2) \rightarrow \pi(5)$ 0.32	
		$\pi(3) \rightarrow 84$ 0.29	
261.8 (4.74)	135	$75 \rightarrow 80$ 0.48	5
		$\pi(2) \rightarrow d(4)$ 0.36	
		$p(1) \rightarrow d(3)$ 0.31	
258.0 (4.81)	66.0	$p(2) \rightarrow d(3)$ 0.44	
		$\pi(2) \rightarrow d(4)$ 0.30	
		$p(1) \rightarrow d(3)$ 0.29	
251.8 (4.92)	371	$\pi(1) \rightarrow d(4)$ 0.54	
		$p(1) \rightarrow d(3)$ 0.31	
		$p(2) \rightarrow d(3)$ 0.18	
247.0 (5.02)	164	$\pi(3) \rightarrow d(4)$ 0.46	
		$p(1) \rightarrow d(3)$ 0.42	
		$\pi(1) \rightarrow d(4)$ 0.26	
239.6 (5.17)	42.0	$p(2) \rightarrow d(4)$ 0.61	
		$\pi(1) \rightarrow d(4)$ 0.21	
		$\pi(2) \rightarrow d(4)$ 0.20	
275.4 (4.50)	3383	$\pi(1) \rightarrow d(3)$ 0.64	4
		$p(2) \rightarrow d(3)$ 0.14	
		$\pi(1) \rightarrow d(4)$ 0.12	
280.7 (4.42)	1.00	$73 \rightarrow 80$ 0.51	3
		$d/p(1) \rightarrow d(3)$ 0.33	
		$d(2) \rightarrow d(3)$ 0.26	
368.0 (3.37)	0.00	$p(3) \rightarrow d(3)$ 0.64	2
		$p(3) \rightarrow d(4)$ 0.23	
		$d(1) \rightarrow d(3)$ 0.11	
361.5 (3.43)	17.0	$\pi(2) \rightarrow d(3)$ 0.67	
		$\pi(3) \rightarrow 85$ 0.12	
		$\pi(3) \rightarrow 84$ 0.11	
350.7 (3.54)	0.00	$p(3) \rightarrow d(4)$ 0.61	
		$p(3) \rightarrow d(3)$ 0.24	
		$\pi(3) \rightarrow d(4)$ 0.20	
311.8 (3.98)	0.00	$\pi(3) \rightarrow d(4)$ 0.61	
		$d/p(1) \rightarrow d(4)$ 0.23	
		$p(3) \rightarrow d(4)$ 0.20	

[†] Diagnostic Λ -value¹ for the transition; Λ is calculated in DALTON² with an ECP for Pt as described in the main paper

TABLE S3: Transitions and assignments for the *trans*-Pt complex, calculated with SR-CAM-B3LYP. In each region (labels **2–6**), the five most intense transitions were selected.

4c				4c			
Energy nm (eV)	Osc. str.($\times 10^{-4}$)	Orbitals (weight)	Interval	Energy nm (eV)	Osc. str.($\times 10^{-4}$)	Orbitals (weight)	Interval
234.8 (5.28)	78.0	$\pi(3) \rightarrow 82$ 0.53	6	306.1 (4.05)	361	$p(2) \rightarrow d(3)$ 0.62	3
		$\pi(3) \rightarrow 84$ 0.34				$\pi(1) \rightarrow d(3)$ 0.31	
		$\pi(2) \rightarrow 87$ 0.19				$p(2) \rightarrow d(4)$ 0.07	
269.3 (4.60)	21.0	$p(1) \rightarrow d(4)$ 0.45	5	393.8 (3.15)	11.0	$\pi(2) \rightarrow d(3)$ 0.70	2
		$p(1) \rightarrow d(3)$ 0.35				$\pi(1) \rightarrow d(3)$ 0.06	
		$p(2) \rightarrow d(4)$ 0.28				$\pi(3) \rightarrow 82$ 0.05	
268.1 (4.62)	13.0	$p(1) \rightarrow d(4)$ 0.49		387.2 (3.20)	0.00	$\pi(3) \rightarrow d(4)$ 0.5552	
		$p(3) \rightarrow d(3)$ 0.34				$p(3) \rightarrow d(4)$ 0.38	
		$\pi(2) \rightarrow d(4)$ 0.25				$d/p(1) \rightarrow d(4)$ 0.13	
267.9 (4.63)	119	$p(1) \rightarrow d(4)$ 0.49		346.0 (3.58)	0.00	$\pi/d(1) \rightarrow d(3)$ 0.64	
		$p(1) \rightarrow d(3)$ 0.32				$\pi(3) \rightarrow d(4)$ 0.15	
		$\pi(2) \rightarrow d(4)$ 0.24				$d/p(1) \rightarrow d(3)$ 0.11	
262.5 (4.72)	74.0	$p(2) \rightarrow d(4)$ 0.62		344.6 (3.60)	0.00	$\pi(3) \rightarrow d(4)$ 0.50	
		$p(1) \rightarrow d(4)$ 0.23				$p(3) \rightarrow d(4)$ 0.40	
		$\pi(1) \rightarrow d(4)$ 0.20				$\pi/d(1) \rightarrow d(3)$ 0.24	
253.4 (4.89)	16.0	$\pi(3) \rightarrow 82$ 0.38		328.7 (3.77)	2.00	$\pi(2) \rightarrow d(4)$ 0.50	
		$\pi(3) \rightarrow 84$ 0.34				$p(1) \rightarrow d(4)$ 0.38	
		$\pi(2) \rightarrow 87$ 0.25				$p(1) \rightarrow d(3)$ 0.18	
294.0 (4.22)	168	$\pi(2) \rightarrow d(4)$ 0.50	4	328.6 (3.77)	2.00	$\pi(2) \rightarrow d(4)$ 0.51	
		$p(2) \rightarrow d(4)$ 0.28				$p(1) \rightarrow d(4)$ 0.38	
		$p(1) \rightarrow d(3)$ 0.24				$p(1) \rightarrow d(3)$ 0.18	
293.0 (4.23)	83.0	$p(2) \rightarrow d(4)$ 0.45		328.4 (3.77)	0.00	$\pi(2) \rightarrow d(4)$ 0.51	
		$p(1) \rightarrow d(3)$ 0.29				$p(1) \rightarrow d(4)$ 0.38	
		$\pi(1) \rightarrow d(4)$ 0.27				$p(1) \rightarrow d(3)$ 0.18	
290.1 (4.27)	1232	$\pi(1) \rightarrow d(3)$ 0.40		437.6 (2.83)	0.00	$\pi(2) \rightarrow d(3)$ 0.54	1
		$\pi(1) \rightarrow d(4)$ 0.38				$\pi(1) \rightarrow d(3)$ 0.43	
		$p(2) \rightarrow d(3)$ 0.27				$\pi(2) \rightarrow d(4)$ 0.06	
287.5 (4.31)	86.0	$p(1) \rightarrow d(3)$ 0.43		436.8 (2.84)	1.00	$\pi(2) \rightarrow d(3)$ 0.51	
		$\pi(2) \rightarrow d(4)$ 0.31				$\pi(1) \rightarrow d(3)$ 0.46	
		$\pi(1) \rightarrow d(4)$ 0.30				$p(2) \rightarrow d(3)$ 0.06	
274.1 (4.52)	1565	$\pi(1) \rightarrow d(4)$ 0.51		435.9 (2.84)	0.00	$\pi(1) \rightarrow d(3)$ 0.53	
		$\pi(1) \rightarrow d(3)$ 0.32				$\pi(2) \rightarrow d(3)$ 0.44	
		$p(2) \rightarrow d(4)$ 0.19				$\pi(3) \rightarrow 84$ 0.07	
435.1 (2.85)	1.00	$\pi(1) \rightarrow d(3)$ 0.52		435.1 (2.85)	1.00	$\pi(1) \rightarrow d(3)$ 0.52	
		$\pi(2) \rightarrow d(3)$ 0.44				$\pi(2) \rightarrow d(3)$ 0.44	
		$p(3) \rightarrow d(4)$ 0.10				$p(3) \rightarrow d(4)$ 0.10	
435.0 (2.85)	0.00	$p(3) \rightarrow d(4)$ 0.52		435.0 (2.85)	0.00	$p(3) \rightarrow d(4)$ 0.52	
		$\pi(3) \rightarrow d(4)$ 0.36				$\pi(3) \rightarrow d(4)$ 0.36	
		$p(3) \rightarrow d(3)$ 0.24				$p(3) \rightarrow d(3)$ 0.24	

TABLE S4: Transitions and assignments for the *trans*-Pt complex, calculated with 4c-B3LYP. In each region (labels **1–6**), the five most intense transitions were selected.

NR			
Energy nm (eV)	Osc. str.($\times 10^{-4}$)	Orbitals (weight)	Interval
299.0 (4.15)	2012	$p(2) \rightarrow d/p(2)$ 0.50	5
		$\pi(2) \rightarrow d(3)$ 0.39	
		$\pi(2) \rightarrow d/p(2)$ 0.22	
294.7 (4.21)	202	$p(2) \rightarrow d/p(2)$ 0.47	
		$\pi(2) \rightarrow d(3)$ 0.37	
		$\pi(2) \rightarrow d/p(2)$ 0.34	
340.0 (3.65)	256	$p(2) \rightarrow d(3)$ 0.64	4
		$\pi(2) \rightarrow d(3)$ 0.27	
		$\pi(2) \rightarrow d/p(2)$ 0.12	
329.8 (3.76)	8.00	$\pi(3) \rightarrow d/p(2)$ 0.62	
		$p(1) \rightarrow d(3)$ 0.31	
		$\pi(2) \rightarrow d(3)$ 0.09	
326.4 (3.80)	536	$\pi(2) \rightarrow d/p(2)$ 0.57	
		$\pi(2) \rightarrow d(3)$ 0.32	
		$p(2) \rightarrow d(3)$ 0.25	
318.1 (3.90)	32.0	$p(1) \rightarrow d(3)$ 0.62	
		$\pi(3) \rightarrow d/p(2)$ 0.29	
		$p(1) \rightarrow d/p(2)$ 0.15	
447.8 (2.77)	8.00	$\pi(3) \rightarrow d(3)$ 0.70	2
		$\pi(2) \rightarrow d(3)$ 0.04	
		$\pi(4) \rightarrow 84$ 0.04	

TABLE S5: Transitions and assignments for the *trans*-Pt complex, calculated with NR-B3LYP. In each region (labels **2**, **4** and **5**), the five most intense transitions were selected.

SR			
Energy nm (eV)	Osc. str.($\times 10^{-4}$)	Orbitals (weight)	Interval
234.3517 (5.29)	77.0	$\pi(3) \rightarrow 82$ 0.53	6
		$\pi(3) \rightarrow \pi(3)$ 0.34	
		$\pi(2) \rightarrow 87$ 0.19	
265.1 (4.68)	103	$p(2) \rightarrow d(4)$ 0.67	5
		$\pi(1) \rightarrow d(4)$ 0.20	
		$\pi(1) \rightarrow d(3)$ 0.06	
295.5 (4.20)	199	$\pi(2) \rightarrow d(4)$ 0.65	4
		$p(1) \rightarrow d(3)$ 0.20	
		$\pi(1) \rightarrow d(3)$ 0.15	
293.5 (4.22)	1.00	$d/\pi(1) \rightarrow d(3)$ 0.58	
		$d/p(1) \rightarrow d(3)$ 0.31	
		$d(2) \rightarrow d(3)$ 0.19	
290.9 (4.26)	1546	$\pi(1) \rightarrow d(3)$ 0.45	(0.3999) [†]
		$\pi(1) \rightarrow d(4)$ 0.42	
		$p(2) \rightarrow d(3)$ 0.28	
280.8 (4.42)	37.0	$p(1) \rightarrow d(3)$ 0.66	
		$\pi(2) \rightarrow d(4)$ 0.19	
		$p(1) \rightarrow d(4)$ 0.13	
275.5 (4.50)	1875	$\pi(1) \rightarrow d(4)$ 0.52	(0.3750) [†]
		$\pi(1) \rightarrow d(3)$ 0.36	
		$p(2) \rightarrow d(4)$ 0.19	
308.2 (4.02)	350	$p(2) \rightarrow d(3)$ 0.63	3
		$\pi(1) \rightarrow 89$ 0.31	
		$\pi(1) \rightarrow d(4)$ 0.06	
397.2 (3.12)	11.0	$\pi(2) \rightarrow d(3)$ 0.70	2
		$\pi(3) \rightarrow 82$ 0.05	
		$\pi(3) \rightarrow 84$ 0.05	

[†] Diagnostic Λ -value¹ for the transition; Λ is calculated in DALTON² with an ECP for Pt as described in the main paper

TABLE S6: Transitions and assignments for the *trans*-Pt complex, calculated with SR-B3LYP. In each region (labels **2–6**), the five most intense transitions were selected.

4c				4c			
Energy nm (eV)	Osc. str.($\times 10^{-4}$)	Orbitals (weight)	Interval	Energy nm (eV)	Osc. str.($\times 10^{-4}$)	Orbitals (weight)	Interval
229.6 (5.40)	89.0	$d(2) \rightarrow d/p(2)$ 0.28 $d(2) \rightarrow d(3)$ 0.26 $p(1) \rightarrow d/p(2)$ 0.23	9	291.1 (4.26)	40.0	$p(3) \rightarrow d/p(2)$ 0.30 $\pi(3) \rightarrow d/p(2)$ 0.25 $\pi(1) \rightarrow d(3)$ 0.23	5
224.4 (5.53)	69.0	$d(2) \rightarrow d/p(2)$ 0.25 $d(1) \rightarrow d(3)$ 0.20 $d(2) \rightarrow d(3)$ 0.20		287.2 (4.32)	6.00	$p(2) \rightarrow d(3)$ 0.34 $p(3) \rightarrow d/p(2)$ 0.27 $\pi(4) \rightarrow d/p(2)$ 0.23	
223.5 (5.55)	69.0	$\pi(3) \rightarrow 85$ 0.24 $d(2) \rightarrow d/p(2)$ 0.21 $d(1) \rightarrow d(3)$ 0.20		282.1 (4.40)	105	$p(3) \rightarrow d/p(2)$ 0.33 $\pi(4) \rightarrow d/p(2)$ 0.26 $p(1) \rightarrow d/p(2)$ 0.21	
217.9 (5.69)	20.0	$d(1) \rightarrow d(3)$ 0.38 $d/p(1) \rightarrow d(3)$ 0.30 $d(2) \rightarrow d(3)$ 0.20		278.7 (4.45)	5.00	$p(1) \rightarrow d/p(2)$ 0.37 $p(2) \rightarrow d/p(2)$ 0.35 $\pi(3) \rightarrow d/p(2)$ 0.19	
213.7 (5.80)	70.0	$d(2) \rightarrow d/p(2)$ 0.25 $\pi(2) \rightarrow 85$ 0.19 $d/p(1) \rightarrow d/p(2)$ 0.17		278.2 (4.46)	17.0	$p(1) \rightarrow d/p(2)$ 0.31 $p(2) \rightarrow d/p(2)$ 0.30 $\pi(3) \rightarrow d/p(2)$ 0.27	
237.5 (5.22)	307	$\pi(2) \rightarrow d/p(2)$ 0.5803 $d(2) \rightarrow d(3)$ 0.12 $\pi(4) \rightarrow \pi(5)$ 0.11	8	327.8 (3.78)	3.00	$\pi(3) \rightarrow d/p(2)$ 0.25 $\pi(3) \rightarrow 86$ 0.24 $\pi(3) \rightarrow \pi(5)$ 0.24	4
236.7 (5.24)	18.0	$\pi(2) \rightarrow d/p(2)$ 0.39 $d(2) \rightarrow d(3)$ 0.34 $p(2) \rightarrow d(3)$ 0.18		323.9 (3.83)	2.00	$\pi(3) \rightarrow \pi(5)$ 0.33 $\pi(3) \rightarrow 86$ 0.28 $p(2) \rightarrow d(3)$ 0.19	
235.0 (5.27)	5.00	$\pi(2) \rightarrow d/p(2)$ 0.40 $d(2) \rightarrow d(3)$ 0.31 $d(1) \rightarrow d(3)$ 0.21		321.6 (3.86)	5.00	$p(2) \rightarrow d(3)$ 0.28 $d(2) \rightarrow d(3)$ 0.24 $p(3) \rightarrow d/p(2)$ 0.21	
234.6 (5.28)	20.0	$\pi(2) \rightarrow d/p(2)$ 0.39 $d(2) \rightarrow d(3)$ 0.30 $d(1) \rightarrow d(3)$ 0.20		313.4 (3.96)	2.00	$\pi(4) \rightarrow 86$ 0.26 $p(2) \rightarrow d(3)$ 0.26 $\pi(4) \rightarrow \pi(5)$ 0.24	
249.1 (4.98)	36.0	$\pi(1) \rightarrow d/p(2)$ 0.25 $\pi(3) \rightarrow 85$ 0.23 $\pi(4) \rightarrow 85$ 0.22	7	310.1 (4.00)	7.00	$p(2) \rightarrow d/p(2)$ 0.36 $p(1) \rightarrow d/p(2)$ 0.34 $\pi(3) \rightarrow d/p(2)$ 0.27	
248.6 (4.99)	4.00	$\pi(4) \rightarrow 85$ 0.25 $\pi(3) \rightarrow 85$ 0.22 $d(2) \rightarrow d/p(2)$ 0.19		305.0 (4.07)	23.0	$p(1) \rightarrow d/p(2)$ 0.34 $\pi(3) \rightarrow d/p(2)$ 0.30 $p(2) \rightarrow d/p(2)$ 0.29	
245.9 (5.04)	38.0	$\pi(1) \rightarrow d/p(2)$ 0.29 $\pi(3) \rightarrow 85$ 0.20 $d(2) \rightarrow d(3)$ 0.19		348.0 (3.56)	9.00	$p(3) \rightarrow d(3)$ 0.54 $\pi(3) \rightarrow d/p(2)$ 0.23 $\pi(2) \rightarrow d(3)$ 0.17	3
245.1 (5.06)	34.0	$d(2) \rightarrow d(3)$ 0.26 $\pi(3) \rightarrow 85$ 0.24 $p(3) \rightarrow d/p(2)$ 0.21		409.9 (3.02)	2.00	$p(3) \rightarrow d/p(2)$ 0.40 $\pi(3) \rightarrow d(3)$ 0.37 $\pi(4) \rightarrow d/p(2)$ 0.23	2
243.8 (5.08)	94.0	$\pi(1) \rightarrow d/p(2)$ 0.43 $d(2) \rightarrow d(3)$ 0.16 $p(1) \rightarrow d/p(2)$ 0.16		392.9 (3.16)	3.00	$p(3) \rightarrow d(3)$ 0.46 $\pi(1) \rightarrow d(3)$ 0.25 $\pi(2) \rightarrow d(3)$ 0.21	
269.2 (4.61)	152	$\pi(1) \rightarrow d(3)$ 0.39 $p(1) \rightarrow d(3)$ 0.31 $p(2) \rightarrow d(3)$ 0.30	6	391.0 (3.17)	2.00	$p(3) \rightarrow d(3)$ 0.49 $\pi(2) \rightarrow d(3)$ 0.29 $\pi(3) \rightarrow d/p(2)$ 0.21	
267.2 (4.64)	211	$p(1) \rightarrow d(3)$ 0.43 $\pi(2) \rightarrow d(3)$ 0.24 $\pi(1) \rightarrow d/p(2)$ 0.17		384.6 (3.22)	2.00	$\pi(1) \rightarrow d(3)$ 0.46 $\pi(3) \rightarrow d/p(2)$ 0.23 $p(3) \rightarrow d/p(2)$ 0.18	
264.8 (4.68)	711	$\pi(2) \rightarrow d(3)$ 0.44 $p(1) \rightarrow d(3)$ 0.28 $p(2) \rightarrow d/p(2)$ 0.21		377.6 (3.28)	2.00	$\pi(2) \rightarrow d(3)$ 0.45 $p(3) \rightarrow d(3)$ 0.29 $\pi(1) \rightarrow d/p(2)$ 0.21	
262.0 (4.73)	389	$\pi(1) \rightarrow d/p(2)$ 0.40 $\pi(2) \rightarrow d(3)$ 0.33 $p(1) \rightarrow d$ 0.23		435.3 (2.85)	7.00	$\pi(4) \rightarrow d(3)$ 0.45 $\pi(4) \rightarrow d/p(2)$ 0.32 $\pi(3) \rightarrow d(3)$ 0.29	1
255.6 (4.85)	194	$p(1) \rightarrow d(3)$ 0.51 $\pi(1) \rightarrow d(3)$ 0.25 $\pi(2) \rightarrow d/p(2)$ 0.21		429.5 (2.89)	2.00	$\pi(3) \rightarrow d(3)$ 0.50 $\pi(4) \rightarrow d/p(2)$ 0.30 $\pi(4) \rightarrow d(3)$ 0.23	

TABLE S7: Transitions and assignments for the *cis*-Pt complex, calculated with 4c CAM-B3LYP. In each region (labels 1–9), the five most intense transitions were selected.

NR							
Energy nm (eV)	Osc. str.($\times 10^{-4}$)	Orbitals (weight)	Interval	Energy nm (eV)	Osc. str.($\times 10^{-4}$)	Orbitals (weight)	Interval
235.2 (5.27)	64.0	$d/p(2) \rightarrow d(2)$ 0.42 $d/p(1) \rightarrow d(2)$ 0.35 $\pi(2) \rightarrow 85$ 0.16	8	325.8 (3.81)	40.0	$\pi(3) \rightarrow d/p(3)$ 0.46 $\pi(2) \rightarrow d/p(3)$ 0.37 $p(2) \rightarrow d/p(3)$ 0.23	4
232.9 (5.32)	614	$p(1) \rightarrow d/p(3)$ 0.37 $d/p(2) \rightarrow d/p(3)$ 0.32 $d/p(1) \rightarrow d/p(3)$ 0.25		311.3 (3.98)	33.0	$p(2) \rightarrow d(2)$ 0.38 $\pi(2) \rightarrow d/p(3)$ 0.32 $\pi(3) \rightarrow d/p(3)$ 0.26	
226.8 (5.47)	384	$d(1) \rightarrow d(2)$ 0.46 $d/p(2) \rightarrow d(2)$ 0.26 $\pi(2) \rightarrow 85$ 0.20		306.9 (4.04)	13.0	$p(2) \rightarrow d(2)$ 0.51 $p(3) \rightarrow d/p(3)$ 0.26 $\pi(2) \rightarrow d/p(3)$ 0.22	
262.1 (4.73)	729	$75 \rightarrow d/p(3)$ 0.53 $\pi(1) \rightarrow d/p(3)$ 0.29 $p(2) \rightarrow d/p(3)$ 0.23	6	385.2 (3.22)	2.00	$p(3) \rightarrow d/p(3)$ 0.48 $p(3) \rightarrow d(2)$ 0.32 $\pi(3) \rightarrow d/p(3)$ 0.27	3
261.0 (4.75)	532	$\pi(1) \rightarrow d/p(3)$ 0.57 $75 \rightarrow d/p(3)$ 0.24 $p(2) \rightarrow d/p(3)$ 0.17		379.8 (3.26)	6.00	$p(3) \rightarrow d(2)$ 0.57 $p(3) \rightarrow d/p(3)$ 0.29 $\pi(2) \rightarrow d/p(3)$ 0.19	
300.2 (4.13)	192	$p(1) \rightarrow d(2)$ 0.56 $75 \rightarrow d(2)$ 0.26 $d(1) \rightarrow d(2)$ 0.15	5	472.2 (2.63)	12.0	$\pi(3) \rightarrow d(2)$ 0.65 $\pi(3) \rightarrow d/p(3)$ 0.21 $p(3) \rightarrow d(2)$ 0.07	1
293.5 (4.22)	1423	$\pi(1) \rightarrow d(2)$ 0.58 $75 \rightarrow d/p(3)$ 0.17 $p(1) \rightarrow d(2)$ 0.16		460.4 (2.69)	5.00	$\pi(2) \rightarrow d(2)$ 0.65 $\pi(2) \rightarrow d/p(3)$ 0.19 $p(3) \rightarrow d(2)$ 0.10	
288.1 (4.30)	372	$75 \rightarrow d/p(3)$ 0.42 $p(2) \rightarrow d/p(3)$ 0.30 $p(1) \rightarrow d/p(3)$ 0.28					
284.4 (4.36)	545	$75 \rightarrow d(2)$ 0.37 $p(1) \rightarrow d/p(3)$ 0.27 $p(2) \rightarrow d/p(3)$ 0.25					

TABLE S8: Transitions and assignments for the *cis*-Pt complex, calculated with NR-CAM-B3LYP. In each region (labels **1**, **3–6** and **8**), the five most intense transitions were selected.

SR							
Energy nm (eV)	Osc. str.($\times 10^{-4}$)	Orbitals (weight)	Interval	Energy nm (eV)	Osc. str.($\times 10^{-4}$)	Orbitals (weight)	Interval
229.9 (5.39)	7.00	$d(2) \rightarrow d(3)$ 0.41	9	299.0 (4.15)	53.0	$p(2) \rightarrow d(3)$ 0.56	5
		$d(1) \rightarrow d(3)$ 0.22				$d(2) \rightarrow d(3)$ 0.27	
		$\pi(4) \rightarrow 83$ 0.17				$\pi(1) \rightarrow d(3)$ 0.20	
227.9 (5.44)	170	$p(1) \rightarrow d/p(2)$ 0.30		285.6 (4.34)	152	$p(3) \rightarrow d/p(2)$ 0.43	
		$d(2) \rightarrow d/p(2)$ 0.26				$\pi(4) \rightarrow d/p(2)$ 0.27	
		$\pi(3) \rightarrow 85$ 0.17				$\pi(1) \rightarrow d(3)$ 0.27	
223.9 (5.54)	174	$d(1) \rightarrow d(3)$ 0.34		309.5 (4.01)	30.0	$\pi(3) \rightarrow d/p(2)$ 0.40	4
		$d(2) \rightarrow d(3)$ 0.30				$\pi(4) \rightarrow d/p(2)$ 0.35	
		$\pi(1) \rightarrow d(3)$ 0.20				$p(2) \rightarrow d/p(2)$ 0.26	
238.1 (5.21)	363	$\pi(2) \rightarrow d/p(2)$ 0.64	8	361.4 (3.43)	3.00	$p(3) \rightarrow d/p(2)$ 0.45	3
		$\pi(4) \rightarrow 84$ 0.12 (0.5210) †				$\pi(4) \rightarrow d/p(2)$ 0.37	
		$\pi(4) \rightarrow 86$ 0.11				$\pi(3) \rightarrow d/p(2)$ 0.26	
246.5 (5.03)	225	$\pi(1) \rightarrow d/p(2)$ 0.61	7	350.1 (3.54)	14.0	$p(3) \rightarrow d(3)$ 0.62	
		$d(2) \rightarrow d/p(2)$ 0.19 (0.5884) †				$\pi(3) \rightarrow d/p(2)$ 0.23	
		$p(1) \rightarrow d/p(2)$ 0.18				$\pi(4) \rightarrow d/p(2)$ 0.11	
271.1 (4.57)	157	$\pi(1) \rightarrow d(3)$ 0.43	6	433.3 (2.86)	12.0	$\pi(4) \rightarrow d(3)$ 0.64	1
		$p(1) \rightarrow d(3)$ 0.31 (0.5054) †				$\pi(4) \rightarrow d/p(2)$ 0.23	
		$p(2) \rightarrow d(3)$ 0.27				$p(3) \rightarrow d(3)$ 0.09	
266.8 (4.65)	1001	$\pi(2) \rightarrow d(3)$ 0.49		425.7 (2.91)	3.00	$\pi(3) \rightarrow d(3)$ 0.64	
		$p(2) \rightarrow d/p(2)$ 0.35 (0.5897) †				$\pi(3) \rightarrow d/p(2)$ 0.22	
		$\pi(3) \rightarrow d/p(2)$ 0.18				$p(3) \rightarrow d(3)$ 0.08	
263.0 (4.71)	576	$\pi(2) \rightarrow d(3)$ 0.40					
		$p(2) \rightarrow d/p(2)$ 0.38 (0.5136) †					
		$p(1) \rightarrow d(3)$ 0.29					
258.4 (4.80)	279	$p(1) \rightarrow d(3)$ 0.53					
		$\pi(1) \rightarrow d(3)$ 0.27 (0.4049) †					
		$p(2) \rightarrow d(3)$ 0.20					

† Diagnostic Λ -value¹ for the transition; Λ is calculated in DALTON² with an ECP for Pt as described in the main paper

TABLE S9: Transitions and assignments for the *cis*-Pt complex, calculated with SR-CAM-B3LYP. In each region (labels **1**, **3–9**), the five most intense transitions were selected.

4c				4c			
Energy nm (eV)	Osc. str.($\times 10^{-4}$)	Orbitals (weight)	Interval	Energy nm (eV)	Osc. str.($\times 10^{-4}$)	Orbitals (weight)	Interval
255.3 (4.86)	62.0	$d(2) \rightarrow d(3)$ 0.24 $d/\pi(1) \rightarrow 87$ 0.21 $d/\pi(1) \rightarrow 83$ 0.21	9	326.9 (3.79)	1.00	$p(2) \rightarrow d(3)$ 0.45 $p(3) \rightarrow d/p(2)$ 0.31 $\pi(1) \rightarrow d(3)$ 0.27	5
254.3 (4.88)	28.0	$d(2) \rightarrow d/p(2)$ 0.27 0. $d/\pi(1) \rightarrow 83$ 0.24 $d/\pi(1) \rightarrow 85$ 0.22		324.3 (3.82)	3.00	$p(1) \rightarrow d/p(2)$ 0.36 $p(2) \rightarrow d/p(2)$ 0.36 $p(3) \rightarrow d/p(2)$ 0.28	
252.7 (4.91)	74.0	$\pi(3) \rightarrow 85$ 0.27 $\pi(3) \rightarrow 83$ 0.22 $\pi(2) \rightarrow d/p(2)$ 0.19		323.8 (3.83)	1.00	$p(1) \rightarrow d/p(2)$ 0.36 $p(2) \rightarrow d/p(2)$ 0.36 $p(3) \rightarrow d/p(2)$ 0.27	
243.2 (5.10)	136	$d(2) \rightarrow d(3)$ 0.33 $d(2) \rightarrow d/p(2)$ 0.26 $p(1) \rightarrow d/p(2)$ 0.22		323.3 (3.83)	1.00	$p(1) \rightarrow d/p(2)$ 0.39 $p(2) \rightarrow d/p(2)$ 0.39 $p(3) \rightarrow d/p(2)$ 0.21	
239.5 (5.18)	200	$d(2) \rightarrow d/p(2)$ 0.32 $d(2) \rightarrow d(3)$ 0.29 $p(1) \rightarrow d/p(2)$ 0.29		319.5 (3.88)	3.00	$p(3) \rightarrow d/p(2)$ 0.55 $p(2) \rightarrow d(3)$ 0.29 $\pi(1) \rightarrow d(3)$ 0.15	
258.5 (4.80)	397	$\pi(2) \rightarrow d/p(2)$ 0.49 $d(2) \rightarrow d(3)$ 0.29 $p(2) \rightarrow d/p(2)$ 0.22	8	349.1 (3.55)	14.0	$\pi(3) \rightarrow d/p(2)$ 0.48 $d/\pi(1) \rightarrow d/p(2)$ 0.26 $p(3) \rightarrow d/p(2)$ 0.24	4
263.9 (4.70)	415	$\pi(1) \rightarrow d/p(2)$ 0.45 $d(2) \rightarrow d(3)$ 0.27 $\pi(2) \rightarrow d/p(2)$ 0.26	7	346.1 (3.58)	7.0	$p(2) \rightarrow d(3)$ 0.37 $\pi(3) \rightarrow d/p(2)$ 0.31 $\pi(2) \rightarrow d(3)$ 0.28	
262.8 (4.72)	2.00	$d(2) \rightarrow d(3)$ 0.52 $\pi(2) \rightarrow d/p(2)$ 0.23 $p(2) \rightarrow d/p(2)$ 0.14		345.4 (3.59)	2.0	$p(2) \rightarrow d(3)$ 0.38 $p(3) \rightarrow d/p(2)$ 0.35 $\pi(2) \rightarrow d(3)$ 0.24	
262.7 (4.72)	44.0	$d(2) \rightarrow d(3)$ 0.48 $\pi(1) \rightarrow d/p(2)$ 0.28 $p(2) \rightarrow d/p(2)$ 0.17		345.3 (3.59)	7.00	$p(2) \rightarrow d(3)$ 0.35 $p(3) \rightarrow d/p(2)$ 0.35 $\pi(2) \rightarrow d(3)$ 0.25	
261.0 (4.75)	106	$d(2) \rightarrow d(3)$ 0.51 $\pi(2) \rightarrow d/p(2)$ 0.24 $p(2) \rightarrow d(3)$ 0.16		331.6 (3.74)	2.00	$p(3) \rightarrow d/p(2)$ 0.38 $p(2) \rightarrow d(3)$ 0.32 $p(2) \rightarrow d/p(2)$ 0.28	
300.1 (4.13)	114	$p(1) \rightarrow d(3)$ 0.38 $\pi(1) \rightarrow d(3)$ 0.38 $\pi(2) \rightarrow d(3)$ 0.22	6	403.0 (3.08)	1.00	$d/\pi(1) \rightarrow d/p(2)$ 0.54 $p(3) \rightarrow d(3)$ 0.18 $p(3) \rightarrow d/p(2)$ 0.18	3
291.4 (4.26)	113	$p(1) \rightarrow d(3)$ 0.59 $\pi(1) \rightarrow d(3)$ 0.22 $p(2) \rightarrow d(3)$ 0.16		396.9 (3.12)	9.00	$p(3) \rightarrow d(3)$ 0.56 $\pi(1) \rightarrow d(3)$ 0.27 $\pi(2) \rightarrow d(3)$ 0.18	
289.9 (4.28)	347	$p(2) \rightarrow d/p(2)$ 0.42 $\pi(2) \rightarrow d(2)$ 0.36 $\pi(2) \rightarrow d/p(2)$ 0.27		388.6 (3.19)	2.00	$\pi(1) \rightarrow d(3)$ 0.46 $p(3) \rightarrow d(3)$ 0.32 $p(2) \rightarrow d(3)$ 0.24	
286.4 (4.33)	415	$\pi(2) \rightarrow d(3)$ 0.37 $p(2) \rightarrow d/p(2)$ 0.35 $\pi(1) \rightarrow d/p(2)$ 0.26		381.5 (3.25)	1.00	$\pi(2) \rightarrow d(3)$ 0.44 $\pi(1) \rightarrow d(3)$ 0.28 $p(2) \rightarrow d(3)$ 0.25	
284.1 (4.36)	100	$\pi(1) \rightarrow d/p(2)$ 0.53 $\pi(2) \rightarrow d(3)$ 0.22 $\pi(2) \rightarrow d/p(2)$ 0.20		428.4 (2.89)	1.00	$p(3) \rightarrow d(3)$ 0.62 $\pi(3) \rightarrow d/p(2)$ 0.26 $\pi(1) \rightarrow d(3)$ 0.10	2
				427.0 (2.90)	4.00	$p(3) \rightarrow d(3)$ 0.60 $\pi(3) \rightarrow d/p(2)$ 0.25 $\pi(3) \rightarrow d(3)$ 0.17	
				426.7 (2.91)	2.00	$p(3) \rightarrow d(3)$ 0.61 $\pi(3) \rightarrow d/p(2)$ 0.27 $\pi(3) \rightarrow d(3)$ 0.14	
				563.1 (2.20)	1.00	$d/\pi(1) \rightarrow d(3)$ 0.67 $\pi(3) \rightarrow d/p(2)$ 0.12 $\pi(3) \rightarrow d(3)$ 0.09	1
				552.0 (2.25)	1.00	$d/\pi(1) \rightarrow d(3)$ 0.66 $\pi(3) \rightarrow d(3)$ 0.15 $d/\pi(1) \rightarrow d/p(2)$ 0.10	
				532.5 (2.33)	1.00	$\pi(3) \rightarrow d(3)$ 0.48 $d/\pi(1) \rightarrow d(3)$ 0.47 $d/\pi(1) \rightarrow d/p(2)$ 0.12	
				474.9 (2.61)	4.00	$d/\pi(1) \rightarrow d(3)$ 0.48 $\pi(3) \rightarrow d(3)$ 0.41 $d/\pi(1) \rightarrow d/p(2)$ 0.28	
				460.5 (2.69)	3.00	$\pi(3) \rightarrow d(3)$ 0.59 $d/\pi(1) \rightarrow d/p(2)$ 0.27 $d/\pi(1) \rightarrow d(3)$ 0.19	

TABLE S10: Transitions and assignments for the *cis*-Pt complex, calculated with 4c-B3LYP. In each region (labels 1–9), the five most intense transitions were selected.

NR			
Energy nm (eV)	Osc. str.($\times 10^{-4}$)	Orbitals (weight)	Interval
8			
244.0 (5.08)	226	$d/p(2) \rightarrow d(2)$ 0.60 $d/p(1) \rightarrow d(2)$ 0.20 $\pi(1) \rightarrow d(2)$ 0.13	
242.4 (5.11)	749	$p(1) \rightarrow d/p(3)$ 0.45 $d/p(2) \rightarrow d/p(3)$ 0.41 $\pi(1) \rightarrow d/p(3)$ 0.15	
6			
279.0 (4.44)	768	$\pi(2) \rightarrow d/p(3)$ 0.55 $\pi(1) \rightarrow d(2)$ 0.23 $d/p(2) \rightarrow d(2)$ 0.19	
275.5 (4.50)	1217	$\pi(1) \rightarrow d/p(3)$ 0.56 $\pi(2) \rightarrow d(2)$ 0.23 $p(2) \rightarrow d/p(3)$ 0.20	
5			
319.5 (3.88)	348	$p(2) \rightarrow d/p(3)$ 0.58 $\pi(2) \rightarrow d(2)$ 0.37 $p(1) \rightarrow d/p(3)$ 0.075	
313.2 (3.96)	630	$\pi(2) \rightarrow d(2)$ 0.41 $\pi(2) \rightarrow d/p(3)$ 0.31 $\pi(1) \rightarrow d(2)$ 0.27	
312.2 (3.97)	549	$\pi(1) \rightarrow d(2)$ 0.46 $\pi(2) \rightarrow d(2)$ 0.31 $\pi(1) \rightarrow d/p(3)$ 0.22	
4			
372.8 (3.33)	29.0	$\pi(2) \rightarrow d/p(3)$ 0.55 $\pi(3) \rightarrow d/p(3)$ 0.38 $p(1) \rightarrow d/p(3)$ 0.10	
358.0 (3.46)	13.0	$p(2) \rightarrow d(2)$ 0.50 $p(3) \rightarrow d/p(3)$ 0.35 $\pi(3) \rightarrow d/p(3)$ 0.20	
353.7 (3.51)	1.00	$p(3) \rightarrow d/p(3)$ 0.46 $p(2) \rightarrow d(2)$ 0.42 $\pi(3) \rightarrow d/p(3)$ 0.19	
332.1 (3.73)	1.00	$p(1) \rightarrow d(2)$ 0.68 $\pi(1) \rightarrow d(2)$ 0.18 $p(2) \rightarrow d/p(3)$ 0.04	
3			
519.4 (2.39)	8.00	$\pi(3) \rightarrow d(2)$ 0.69 $\pi(3) \rightarrow d/p(3)$ 0.11 $\pi(2) \rightarrow d/p(3)$ 0.04	
504.0 (2.46)	3.00	$\pi(2) \rightarrow d(2)$ 0.69 $\pi(2) \rightarrow d/p(3)$ 0.10 $\pi(3) \rightarrow d/p(3)$ 0.07	
442.4 (2.80)	7.00	$p(3) \rightarrow d(2)$ 0.70 $\pi(3) \rightarrow d/p(3)$ 0.07 $\pi(2) \rightarrow d(2)$ 0.04	
418.2 (2.96)	1.00	$\pi(3) \rightarrow d/p(3)$ 0.49 $p(3) \rightarrow d/p(3)$ 0.38 $\pi(2) \rightarrow d/p(3)$ 0.29	

TABLE S11: Transitions and assignments for the *cis*-Pt complex, calculated with NR-B3LYP. In each region (labels **1–6**), the five most intense transitions were selected.

SR				SR			
Energy nm (eV)	Osc. str.($\times 10^{-4}$)	Orbitals (weight)	Interval	Energy nm (eV)	Osc. str.($\times 10^{-4}$)	Orbitals (weight)	Interval
9				6			
242.7 (5.11)	19.0	$d/\pi(2) \rightarrow 82$ 0.62 $d/\pi() \rightarrow 82$ 0.23 $\pi/p(1) \rightarrow 82$ 0.14		298.8 (4.15)	280	$\pi(1) \rightarrow d(3)$ 0.53 $p(1) \rightarrow d(3)$ 0.26 $p(2) \rightarrow d(3)$ 0.19	(0.5872) †
241.1 (5.14)	91.0	$d(2) \rightarrow d(3)$ 0.54 $d/\pi(1) \rightarrow 82$ 0.20 $d/\pi(2) \rightarrow 83$ 0.16		294.5 (4.21)	72.0	$p(1) \rightarrow d(3)$ 0.65 $\pi(1) \rightarrow d(3)$ 0.19 $p(2) \rightarrow d(3)$ 0.12	
238.9 (5.19)	352	$p(1) \rightarrow d/p(2)$ 0.44 $d(2) \rightarrow d/p(2)$ 0.31 $d/\pi(2) \rightarrow 82$ 0.18		291.0 (4.26)	254	$p(2) \rightarrow d/p(2)$ 0.55 $\pi(2) \rightarrow d(3)$ 0.28 $\pi(2) \rightarrow d/p(2)$ 0.21	(0.5578) †
8				5			
258.8 (4.79)	468	$\pi(2) \rightarrow d/p(2)$ 0.60 $d(2) \rightarrow d(3)$ 0.20 $p(2) \rightarrow d/p(2)$ 0.18	(0.5694) †	287.8 (4.31)	743	$\pi(2) \rightarrow d(3)$ 0.52 $p(2) \rightarrow d/p(2)$ 0.29 $\pi(1) \rightarrow d/p(2)$ 0.27	(0.5402) †
7				4			
263.7 (4.70)	662	$\pi(1) \rightarrow d/p(2)$ 0.59 $p(2) \rightarrow d/p(2)$ 0.19 $d(2) \rightarrow d/p(2)$ 0.17	(0.5815) †	322.0 (3.85)	6.00	$\pi/p(1) \rightarrow d/p(2)$ 0.61 $p(2) \rightarrow d(3)$ 0.22 $d/\pi(2) \rightarrow d/p(2)$ 0.19	
3				1			
351.2 (3.53)	25.0	$d/\pi(1) \rightarrow d/p(2)$ 0.62 $d/\pi(2) \rightarrow d/p(2)$ 0.23 $\pi/p(1) \rightarrow d(3)$ 0.14		397.4 (3.12)	7.00	$\pi/p(19) \rightarrow 80$ 0.59 $d/\pi(2) \rightarrow d/p(2)$ 0.36 $\pi/p(1) \rightarrow d/p(2)$ 0.12	
331.3 (3.74)	2.00	$p(2) \rightarrow d(3)$ 0.58 $\pi(1) \rightarrow d(3)$ 0.23 $\pi/p(1) \rightarrow d/p(2)$ 0.22		394.6 (3.14)	6.00	$d/\pi(2) \rightarrow d/p(2)$ 0.48 $\pi/p(1) \rightarrow d(3)$ 0.36 $d/\pi(1) \rightarrow d/p(2)$ 0.25	
480.5 (2.58)	6.00	$d/\pi(2) \rightarrow d(3)$ 0.69 $d/\pi(2) \rightarrow d/p(2)$ 0.08 $d/\pi(1) \rightarrow d/p(2)$ 0.08		461.9 (2.68)	4.00	$d/\pi(29) \rightarrow d(3)$ 0.68 $d/\pi(2) \rightarrow d/p(2)$ 0.14 $d/\pi(1) \rightarrow d/p(2)$ 0.08	

† Diagnostic Λ -value¹ for the transition; Λ is calculated in DALTON² with an ECP for Pt as described in the main paper

TABLE S12: Transitions and assignments for the *cis*-Pt complex, calculated with SR-B3LYP. In each region (labels **1** and **3–9**), the five most intense transitions were selected.

ORBITAL FOR CAM-B3LYP CALCULATIONS

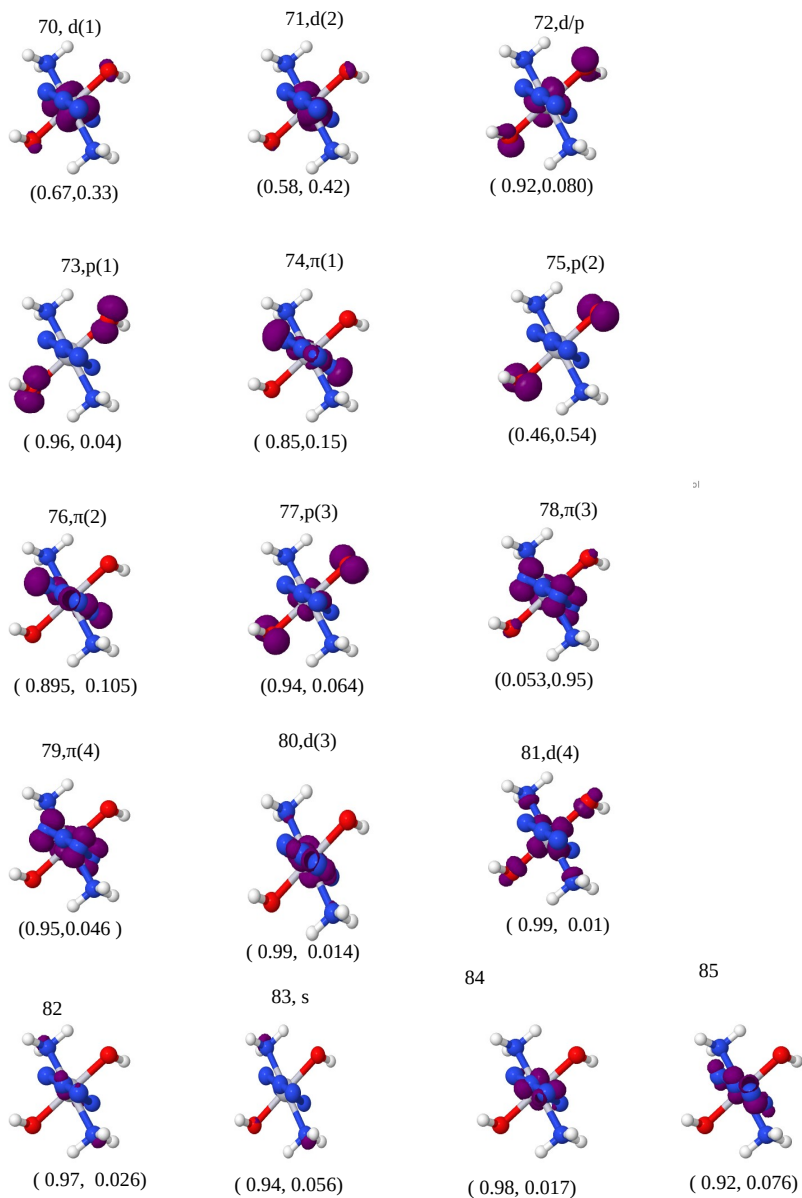


FIG. S1: Orbital densities for *trans*-Pt, computed with 4c-CAM-B3LYP. Numbers below the orbital densities are α - and β -occupations, respectively.

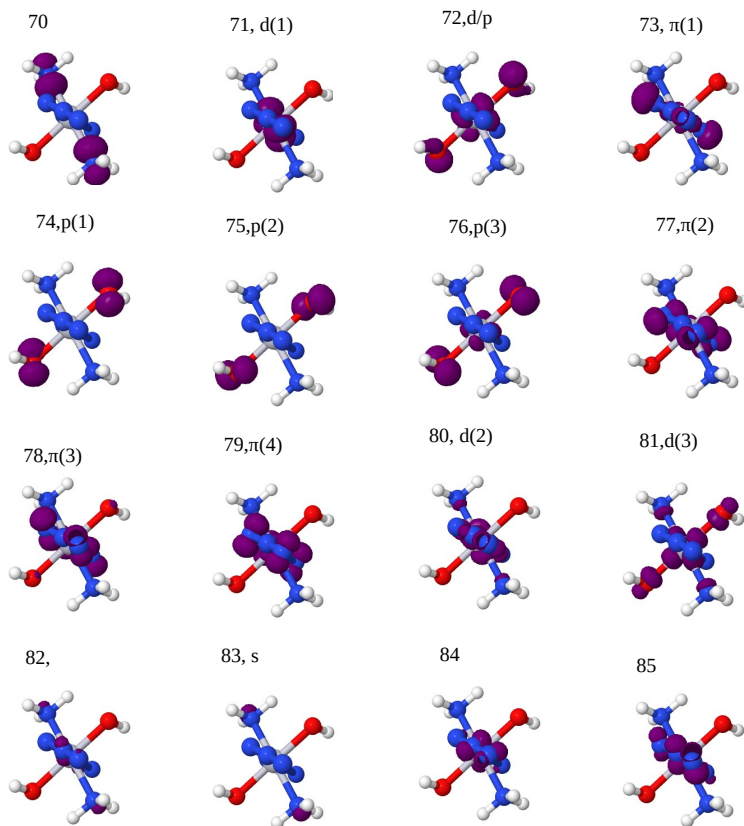


FIG. S2: Orbital densities for *trans*-Pt, computed with NR-CAM-B3LYP.

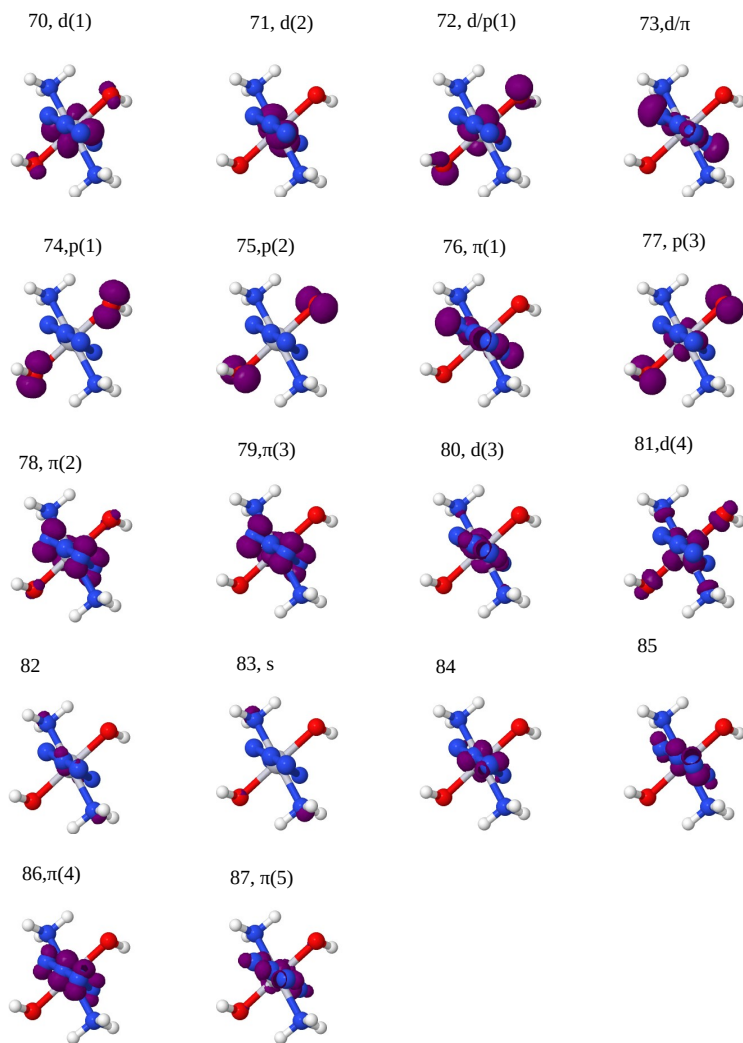


FIG. S3: Orbitals densities for *trans*-Pt, computed with SR-CAM-B3LYP.

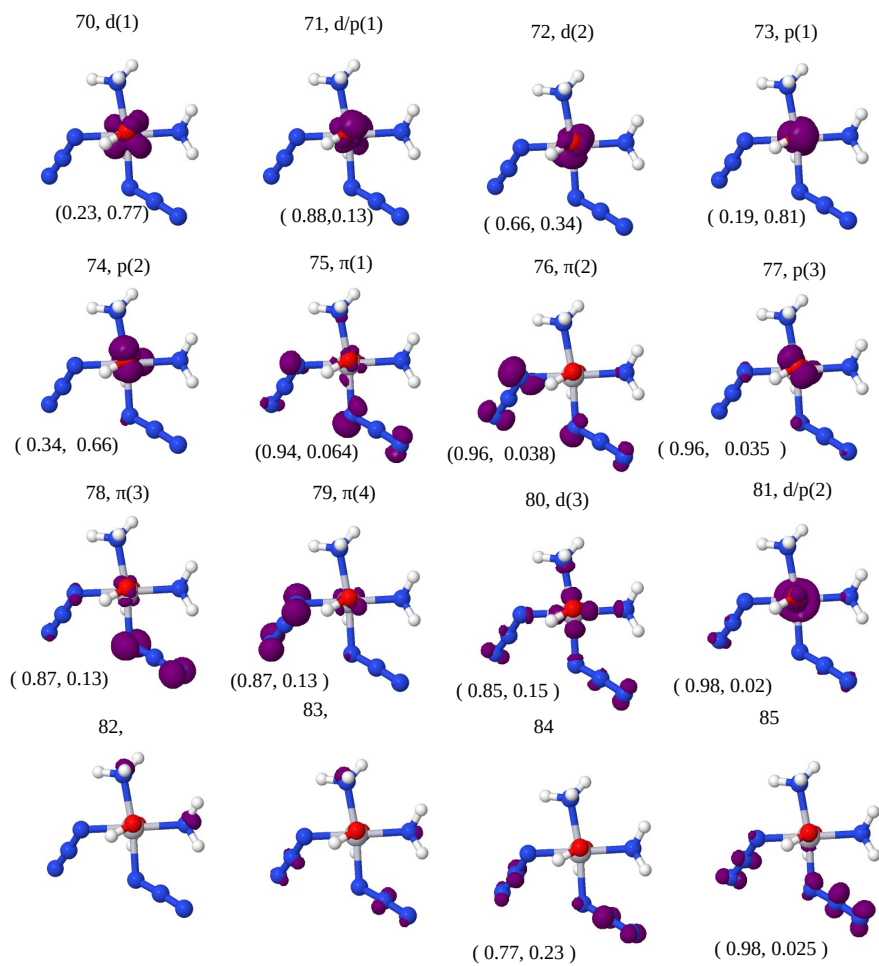


FIG. S4: Orbital densities for *cis*-Pt, computed with 4c-CAM-B3LYP. Numbers below the orbital densities are α - and β -occupations, respectively.

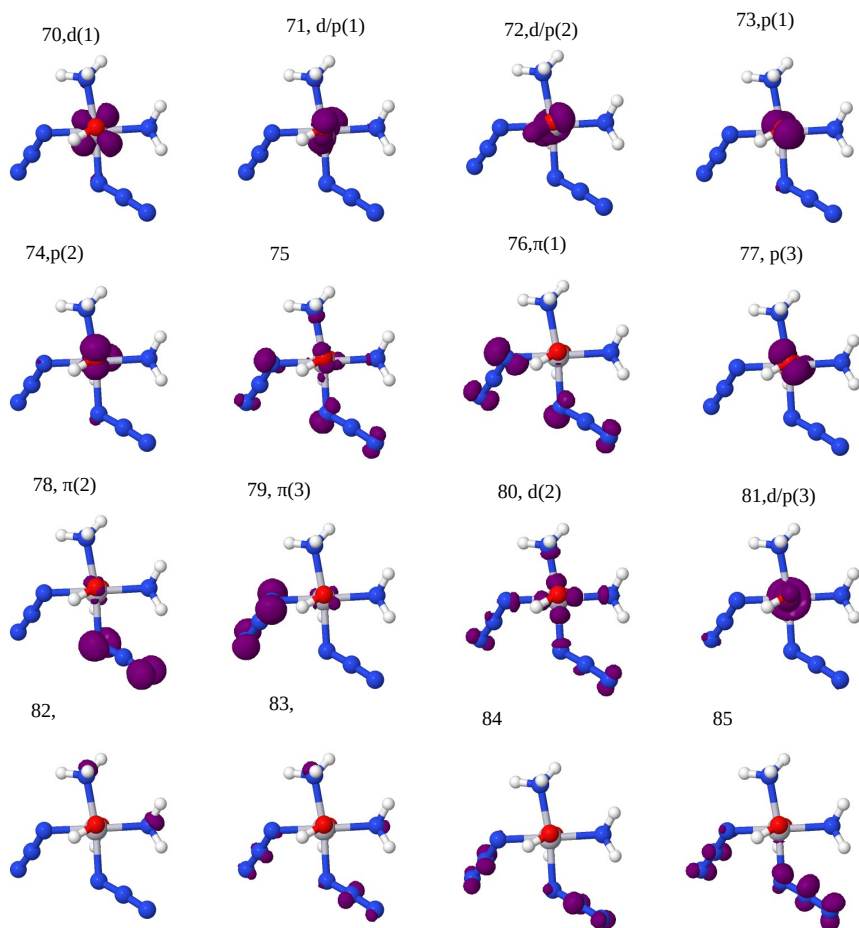


FIG. S5: Orbital densities for *cis*-Pt, computed with NR-CAM-B3LYP.

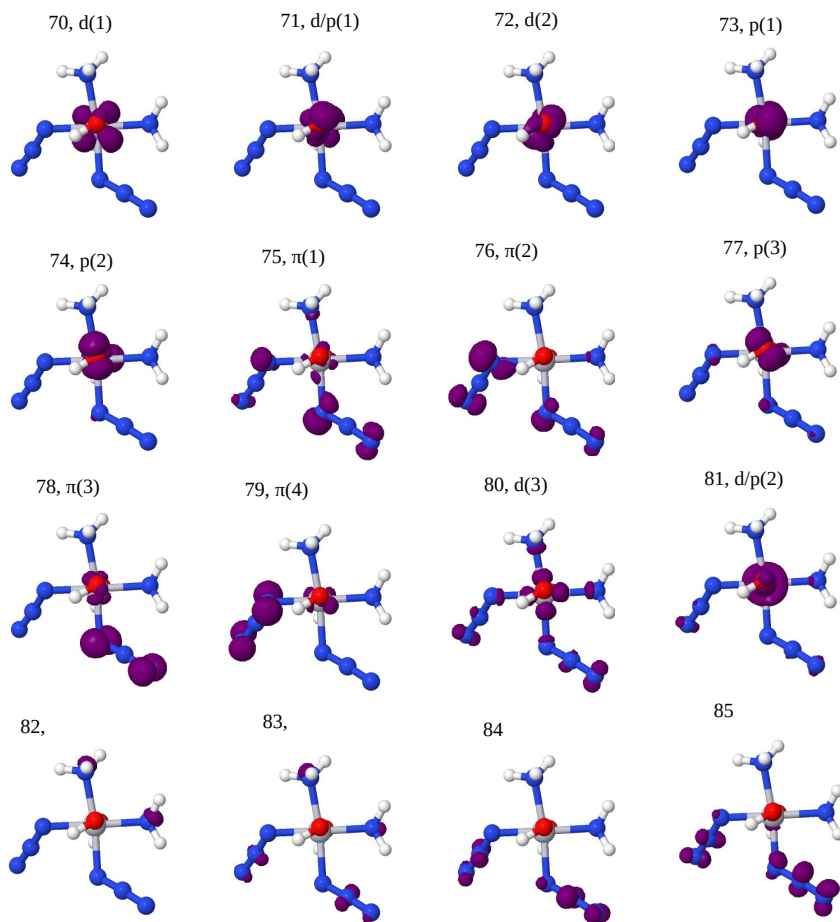


FIG. S6: Orbital densities for *cis*-Pt, computed with SR-CAM-B3LYP.

ORBITALS FOR B3LYP CALCULATIONS

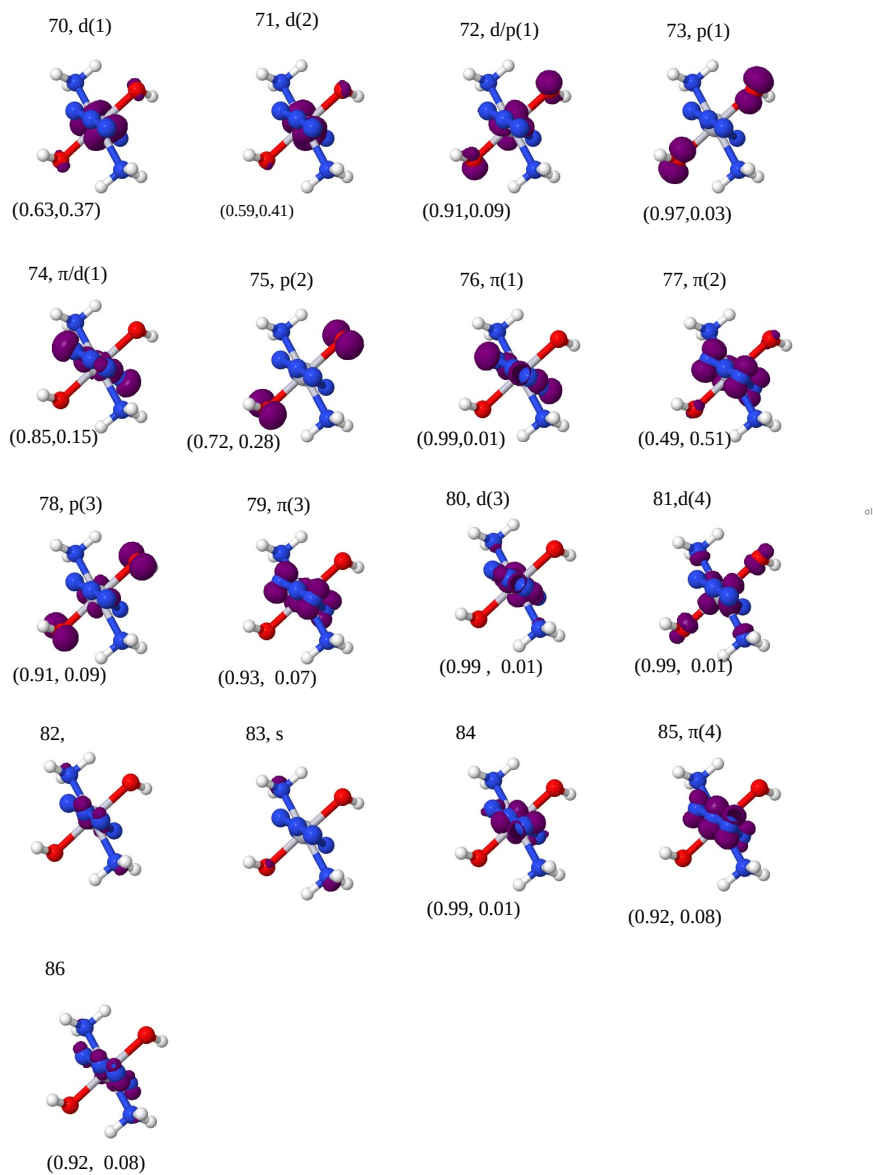


FIG. S7: Orbital densities for *trans*-Pt, computed with 4c-B3LYP. Numbers below the orbital densities are α - and β -occupations, respectively.

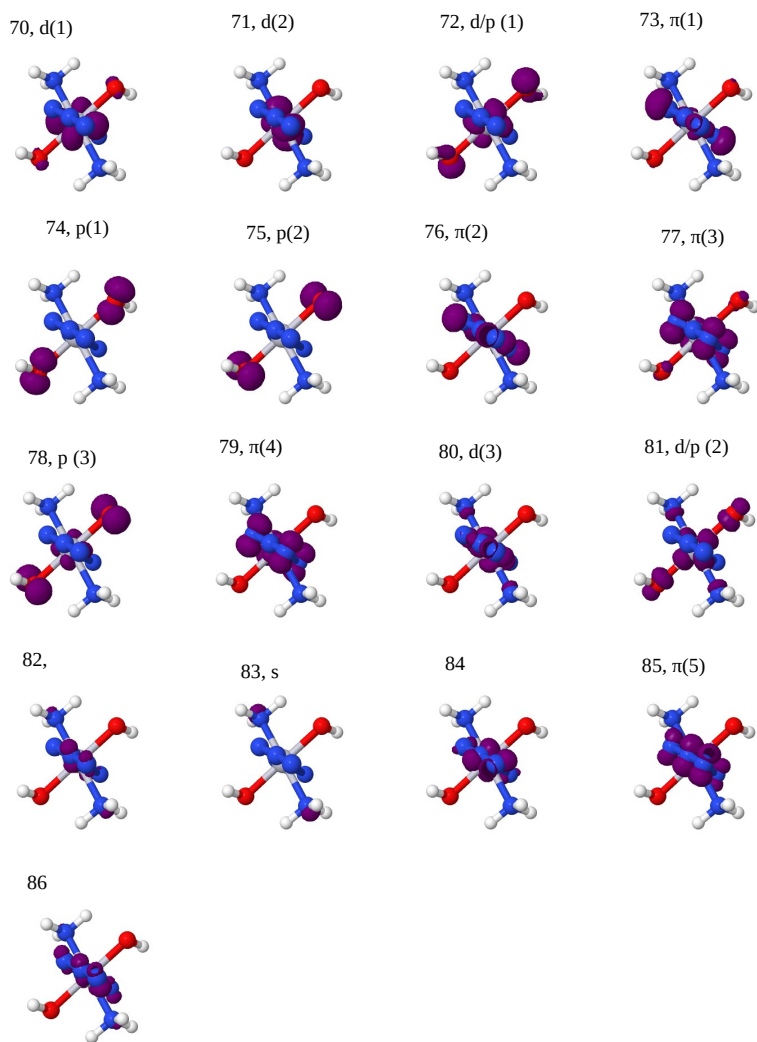


FIG. S8: Orbital densities for *trans*-Pt, computed with NR-B3LYP.

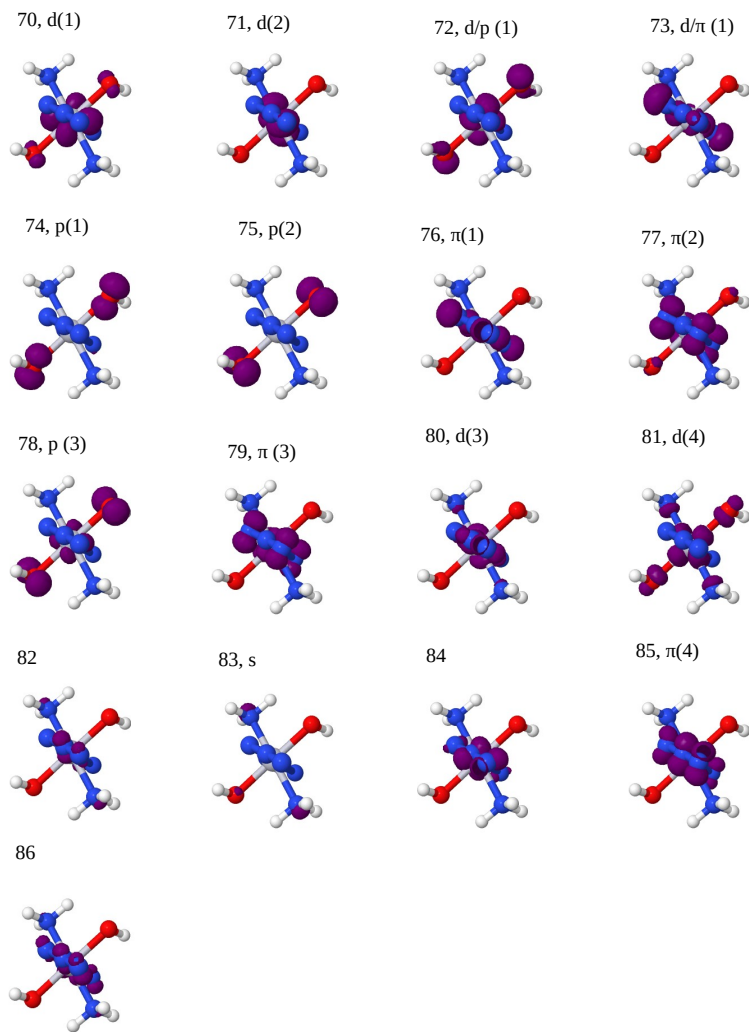


FIG. S9: Orbital densities for *trans*-Pt, computed with SR-B3LYP.

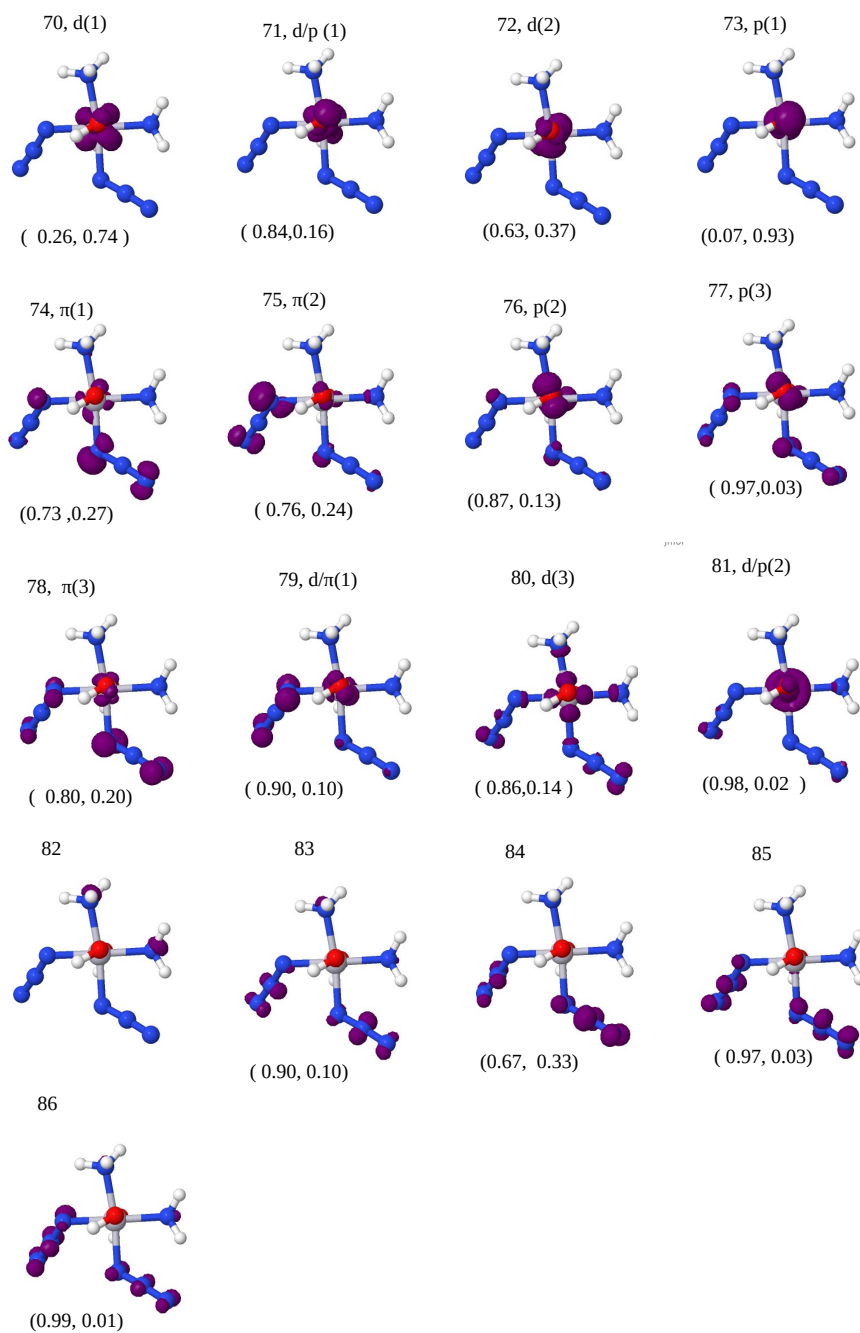


FIG. S10: Orbital densities for *cis*-Pt, computed with 4c-B3LYP. Numbers below the orbital densities are α - and β -occupations, respectively.

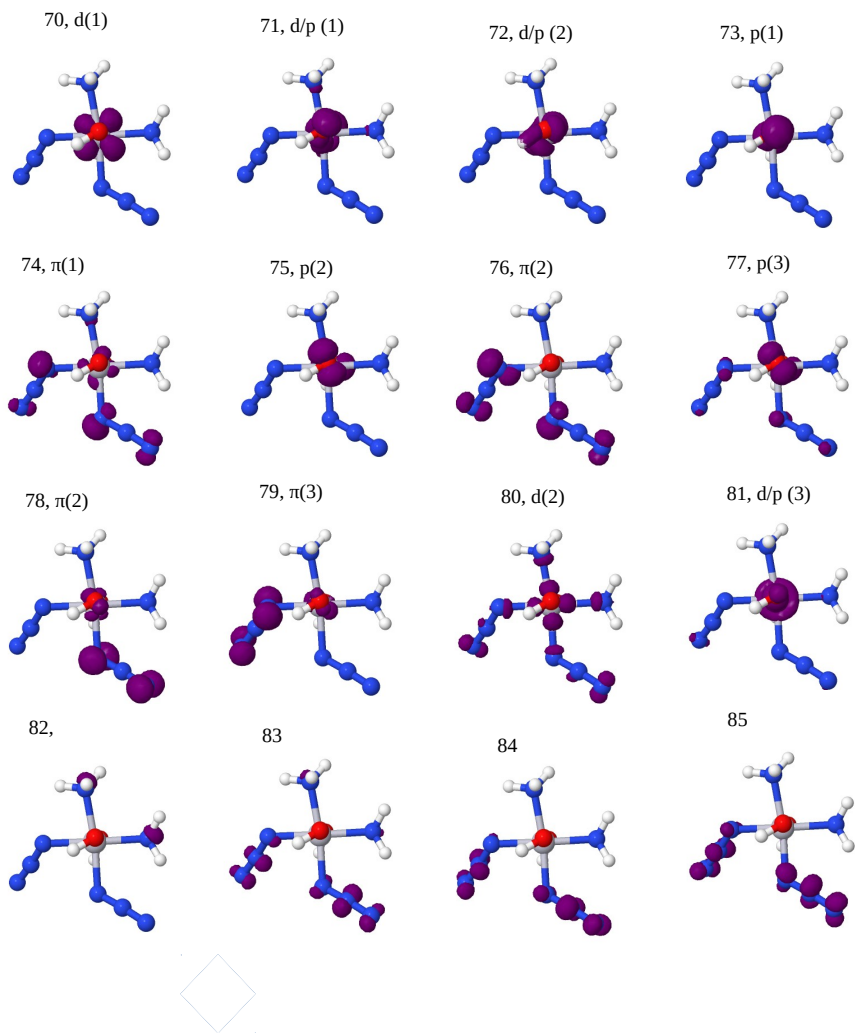


FIG. S11: Orbital densities for *cis*-Pt, computed with NR-B3LYP.

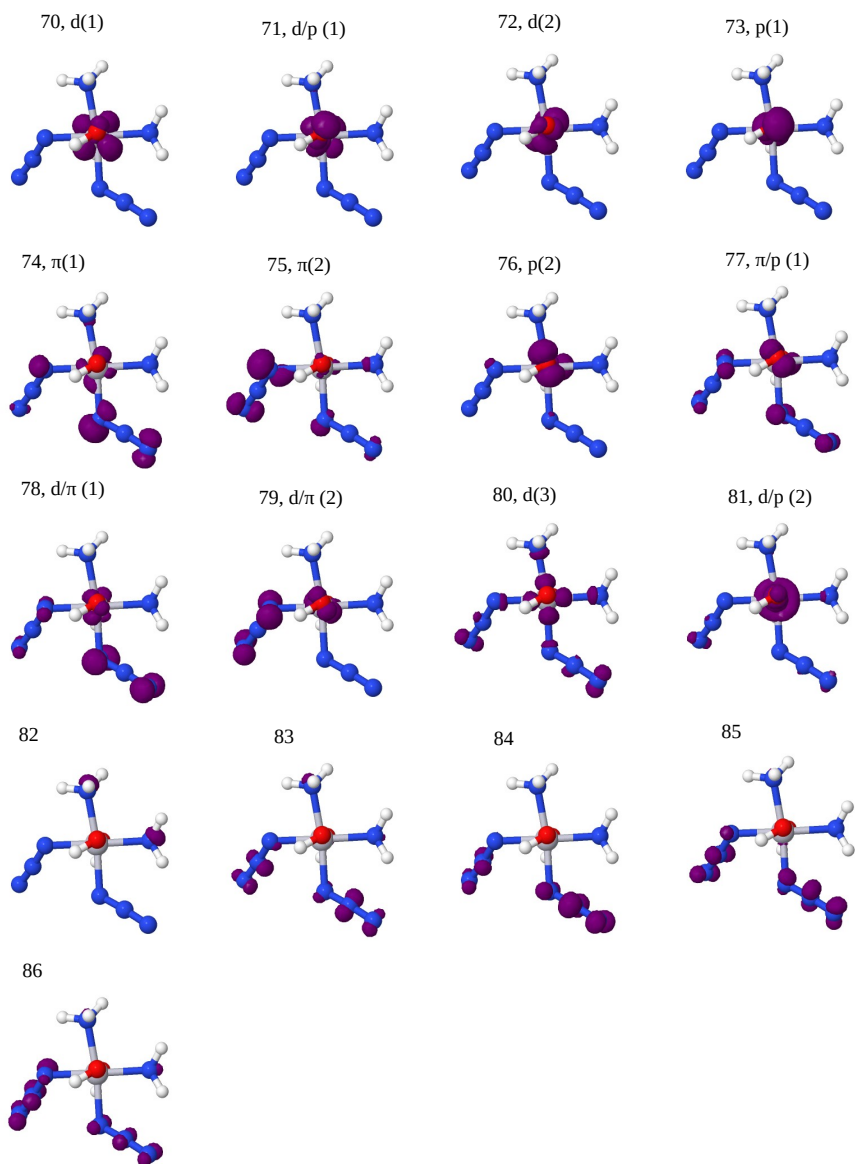


FIG. S12: Orbital densities for *cis*-Pt, computed with SR-B3LYP.

NON-RELATIVISTIC CALCULATIONS

The *trans*-Pt complex

The spectra calculated in 4c and NR frameworks are compared in Figure S13. It is apparent that spectra from NR and 4c frameworks are rather different. Due to the neglect

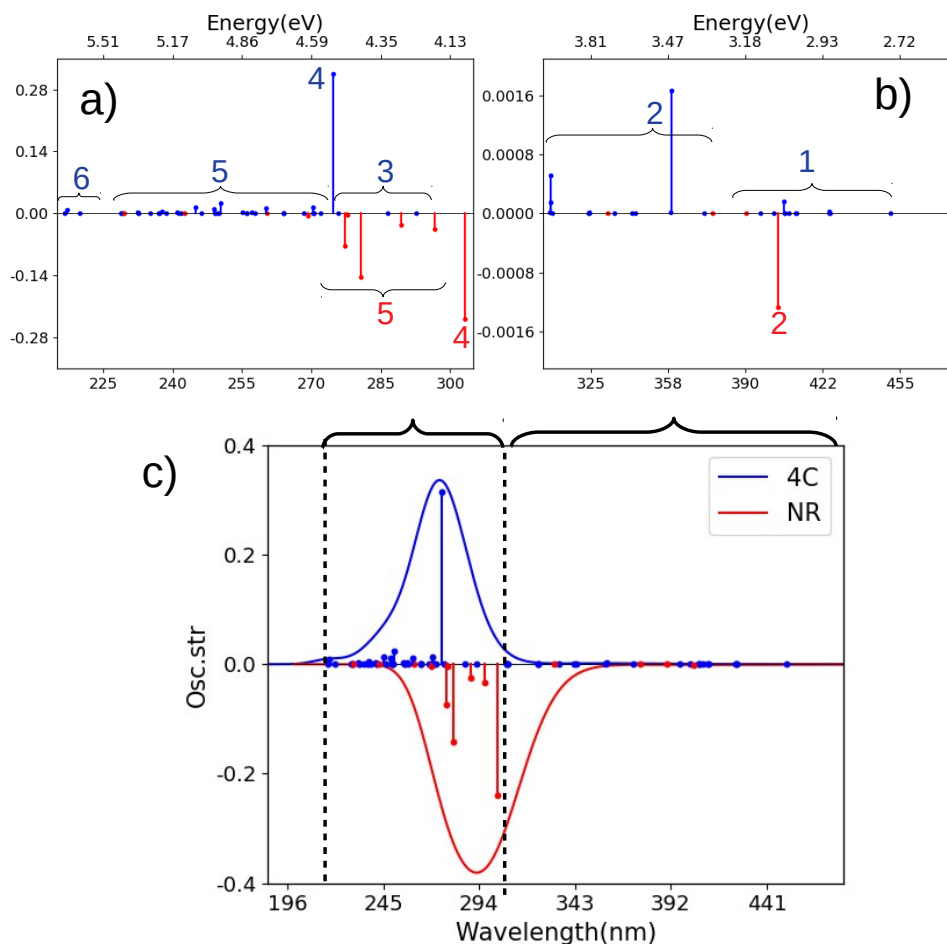


FIG. S13: Spectra for *trans*-Pt calculated with CAM-B3LYP and NR or 4c Hamiltonians. (a) and (b) are magnified for 215–305 nm and 305–480 nm. (c) shows the full spectrum. Assignments of main transitions within regions **1–6** are provided in Tables S1 and S2.

of spin-orbit coupling, the density of states is generally lower in the NR calculation and few transitions occur between 5.7–4.6 eV (i.e. in what corresponds to regions **6** and **5** in the 4c calculation). Rather, the transitions labeled **5** for the NR calculation appear somewhat red-shifted at 4.47–4.18 eV (277–297 nm) and with much higher intensity. In the NR calculation, the transition with highest intensity in region **5** (4.42 eV or 281 nm) primarily involves

orbitals on oxygen and the metal center ($p \rightarrow d$), but otherwise the transitions in **5** have compositions similar to those in the 4c calculation (i.e. mixture of $\pi \rightarrow d$ and $p \rightarrow d$, cf. Table S2).

The transitions labeled **4** are intense, just as in the 4c framework, and corresponds also to a transition of $\pi \rightarrow d$ character (cf. Table S2). As seen from Figure S13 (a) the NR calculation is again red-shifted (4.09 eV or 303 nm, compared to 4.51 eV or 275 nm in the 4c case).

Moving to the lower-energy transitions in Figure S13 (b), no transitions in the NR calculation match the (mainly $\pi \rightarrow d$) transitions in region **1** around 3.08–2.75 eV (402–451 nm) in the 4c calculation. Region **2** is also quite different in 4c and NR frameworks: in the former, the region is a mixture of $\pi \rightarrow d$ and $p \rightarrow d$ transitions of which the most intense (at 3.46 eV or 358 nm) is of $\pi \rightarrow d$ character. Only one transition is seen in the NR framework (also of $\pi \rightarrow d$ character), but is considerable red shifted compared to the 4c counterpart (3.07 eV or 404 nm, compared to 4.03–3.46 eV or 308–359 nm).

For the B3LYP calculation in Figure S14 we see that despite the differences between the B3LYP and the range-separated variant, the changes between 4c-B3LYP and NR-B3LYP calculations are qualitatively the same as seen for CAM-B3LYP. Thus, the density of states is (as expected) much lower for the spectra calculated in the NR and SR frameworks. Further, for region **5** the transitions in NR-B3LYP are much more intense than predicted by the corresponding 4c calculation and also considerably red-shifted (4.21–4.14 vs. 4.60–4.89 eV). Yet, the character of the transitions in region **5** (a mix of $\pi \rightarrow d$ and $p \rightarrow d$) is the same in both 4c and NR frameworks. Meanwhile, in region **4** the intense transitions are red-shifted (as for CAM-B3LYP); they appear at 4.52–4.21 eV (274–294 nm) and 3.90–3.65 eV (318–340 nm) in 4c- and NR-B3LYP calculations, respectively. Also here, the character of the transition is the same, i.e. comprised mostly of $\pi \rightarrow d$ transitions and to less degree of $p \rightarrow d$ transitions (cf. Table S4).

The *cis*-Pt complex

The spectra obtained with 4c and NR frameworks are shown in Figure S15. The full spectra are shown in Figure S15 (c) and it can from this figure be seen that also for *cis*-Pt, the NR calculation varies considerably from the 4c calculation. The transitions at highest

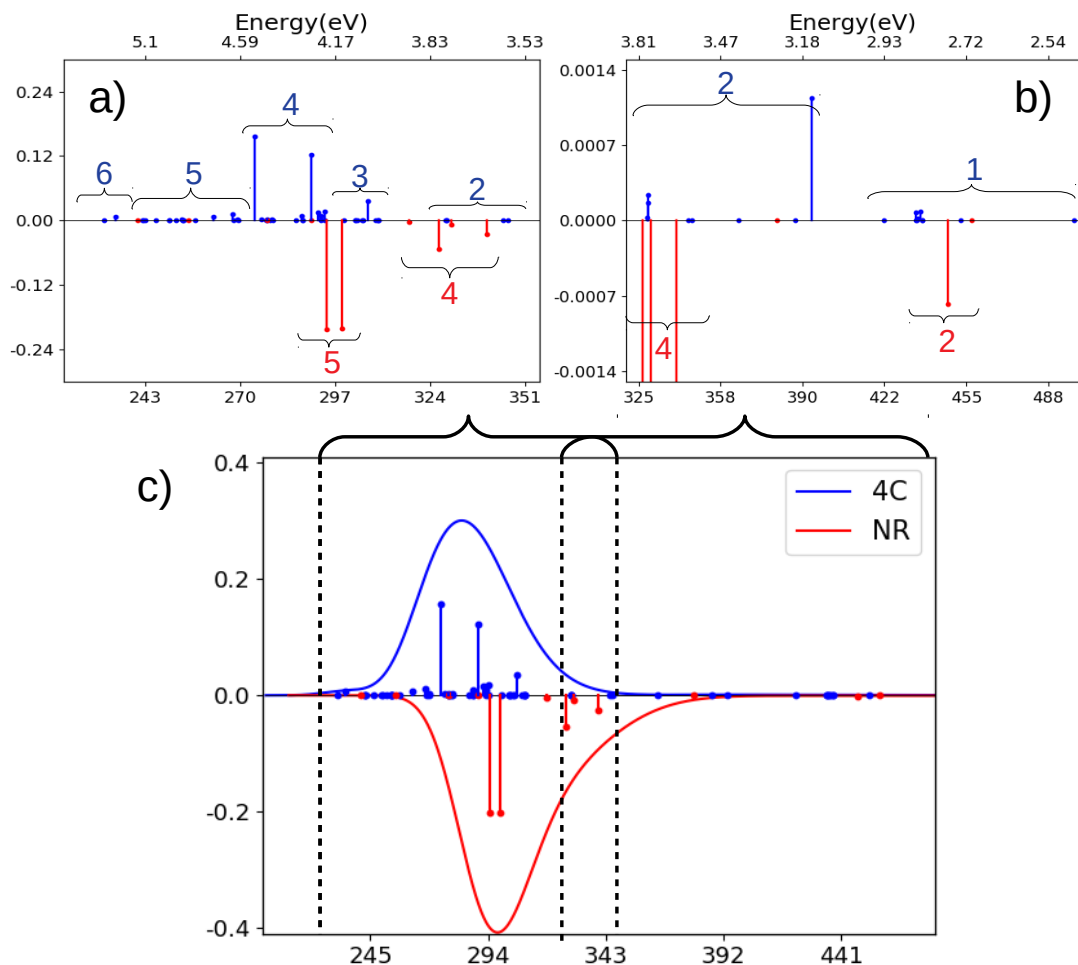


FIG. S14: Spectra for *trans*-Pt calculated with B3LYP and NR or 4c Hamiltonians. (a) and (b) are magnified for 220–355 nm and 328–500 nm. (c) shows the full spectrum. Assignments of main transitions within regions **1–6** are provided in Tables S4 and S5.

energy are qualitatively different in the NR calculation compared the 4c counterparts: we only see few transitions (of $d \rightarrow d$ character) at these high energies: they occur at 5.47–5.27 eV or 227–235 nm and are labeled **8** in Figure S15 (a).

As the 4c calculations, the NR calculation also has intense transitions in regions **6** and **5** with similar character (apart from the lower density of states): region **6** is at 4.75–4.73 eV (261–262 nm) and **5** is at 4.36–4.13 eV (284–300 nm); the transitions at **5** generally have considerably higher intensity compared to 4c counterpart.

Regions **4** and **3** have similar characters as the 4c calculation, but **3** is significantly red-shifted (at 3.26–3.22 eV or 380–385 nm). Interestingly, region **2** in the 4c calculation consists

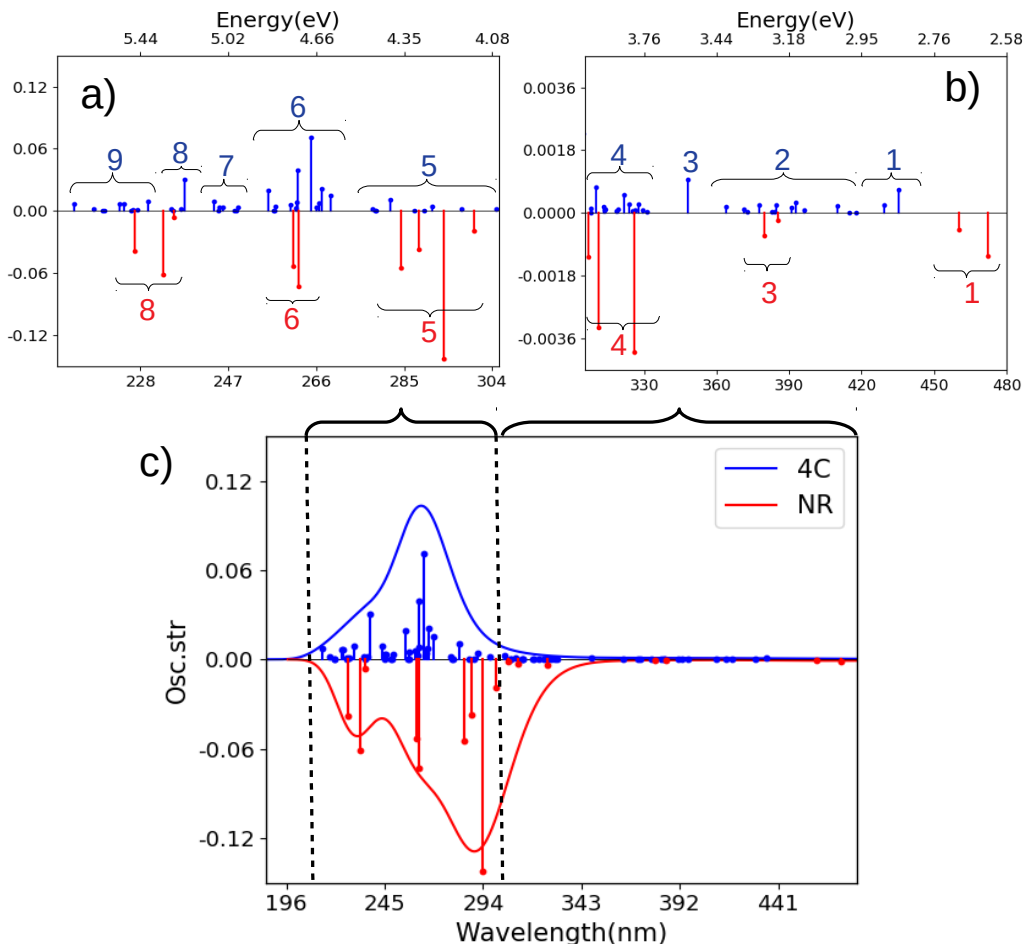


FIG. S15: Spectra for *cis*-Pt calculated with CAM-B3LYP and NR or 4c Hamiltonians. (a) and (b) are magnified for 210–306 nm and 306–480 nm. (c) shows the full spectrum. Assignments of main transitions within regions **1–9** are provided in Tables S7 and S8.

of many low-intensity LMCT transitions (of mixed $\pi \rightarrow d$ and $p \rightarrow p$ character) at 3.28–3.02 eV (378–410 nm), but no match is found in the NR calculations. The last region (**1**) is of LMCT character ($\pi \rightarrow d$, similar to the 4c calculation), and is also red-shifted (2.69–2.62 eV or 460–472 nm compared to 2.89–2.84 eV or 430–435 nm in the 4c calculation). With respect to the B3LYP results (FIG. S16), the two functionals yield qualitatively similar spectra: as seen for NR-CAM-B3LYP, the NR-B3LYP calculation shows intense transitions in regions **8**, **6** and **5** and the character of the underlying transitions are similar, although the three regions also for NR-B3LYP are red-shifted with 0.2–0.5 eV, compared to NR-CAM-B3LYP. The NR-B3LYP calculation also overestimates the intensities in region **5** compared to the

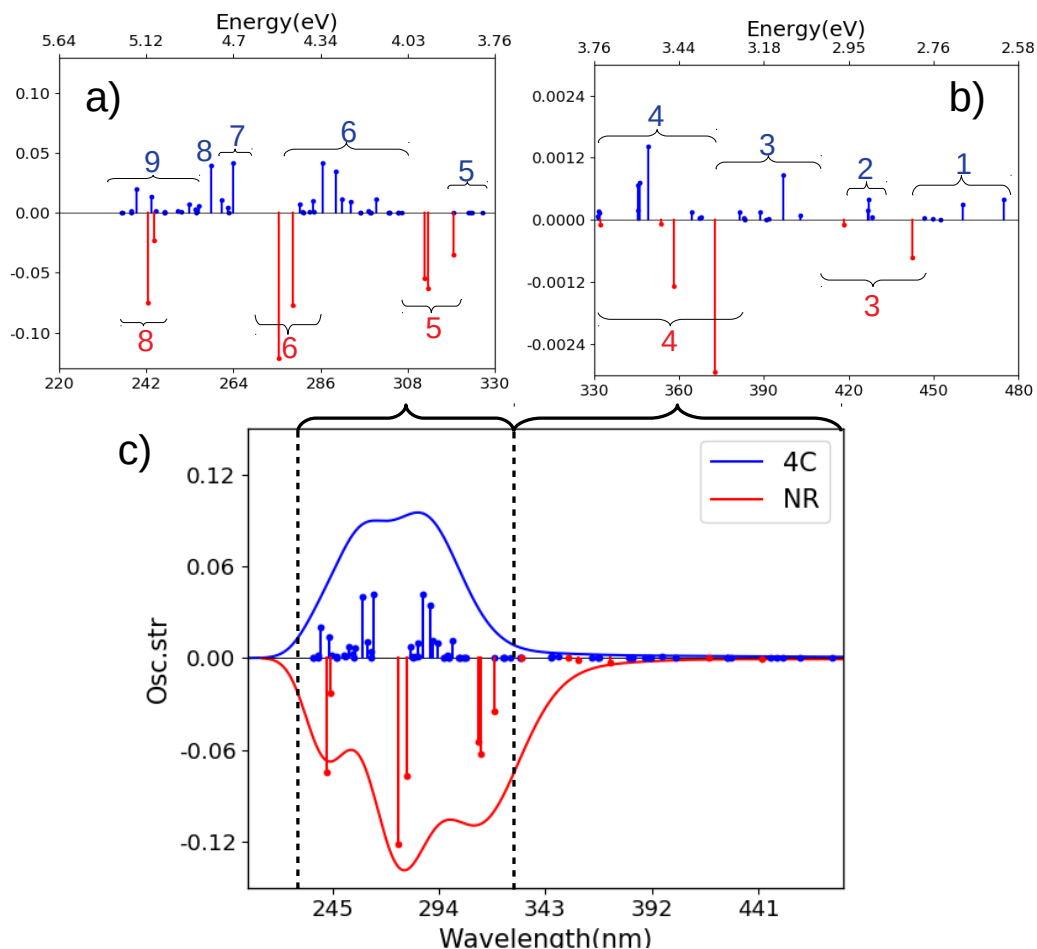


FIG. S16: Spectra for *cis*-Pt calculated with B3LYP and NR or 4c Hamiltonians. (a) and (b) are magnified for 220–330 nm and 330–480 nm. (c) shows the full spectrum. Assignments of main transitions within regions 1–9 are provided in Tables S10 and S11.

relativistic counterparts (as seen with CAM-B3LYP).

For regions 4–1 in Figure S16, B3LYP obtained a energy shift (around 0.5–0.2 eV) to the same regions in the CAM-B3LYP calculation, as seen for the high-energy parts (this was also seen in the 4c calculations). As for the 4c -B3LYP calculations, NR-B3LYP calculations obtain roughly the same character for the transitions ($p \rightarrow d$ and $\pi \rightarrow d$ character). However, region 1 ($\pi \rightarrow d$ for 4c and NR-CAM-B3LYP) is not seen for NR-B3LYP.

RESULTS WITH EFFECTIVE CORE POTENTIALS

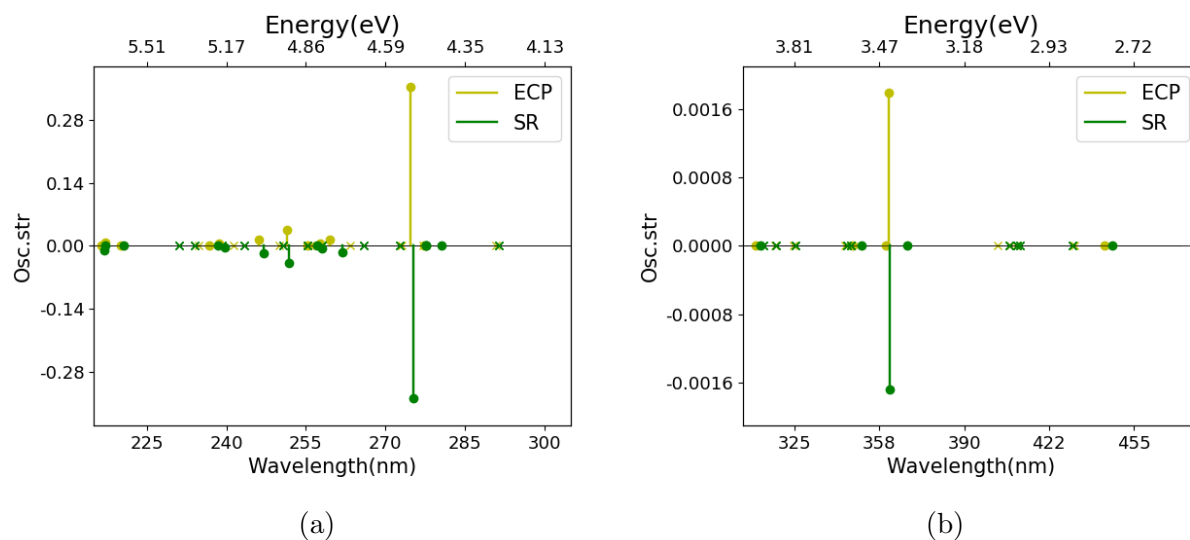


FIG. S17: Spectra for *trans*-Pt calculated with CAM-B3LYP with a non-relativistic Hamiltonian and an ECP (aug-cc-pVDZ-PP) compared against SR.

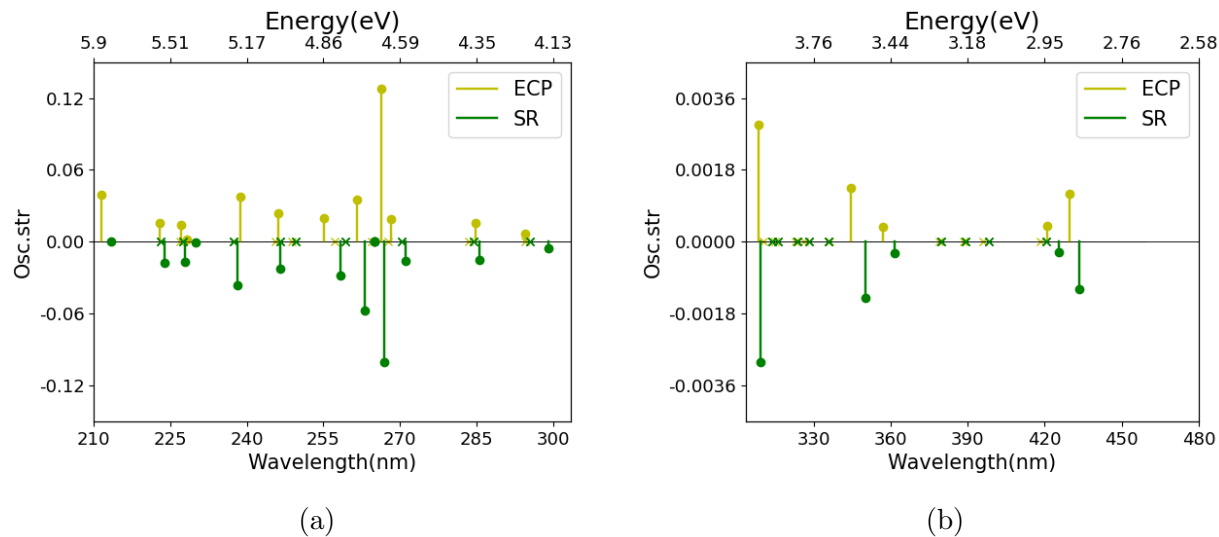


FIG. S18: Spectra for *cis*-Pt calculated with CAM-B3LYP with a non-relativistic Hamiltonian and an ECP (aug-cc-pVDZ-PP), compared against SR.

OPTIMIZED STRUCTURES

trans-trans-trans [Pt(N3)2(OH)2(NH3)2]

Pt	0.0030296	0.0804983	-0.0126311
N	2.0467267	0.4167976	0.0494694
N	-0.1076269	2.0460916	-0.7470400
N	-2.0405459	-0.2549888	-0.0732079
N	0.1135228	-1.8852251	0.7208386
O	0.2137166	0.7174014	1.9274072
O	-0.2096251	-0.5585960	-1.9520748
H	0.1045737	-0.0995678	2.4669045
H	-0.1022309	0.2570469	-2.4937938
N	-1.1336797	2.6361105	-0.4383698
H	2.6362939	-0.3966937	-0.1903809
H	2.2900612	1.2298226	-0.5382408
H	2.1348716	0.6725786	1.0579852
N	1.1337565	-2.4803873	0.4023736
N	2.0930545	-3.0822423	0.1474707
H	-2.1274981	-0.5177303	-1.0801558
H	-2.2853544	-1.0630383	0.5206816
H	-2.6291991	0.5612755	0.1597674
N	-2.0988469	3.2323466	-0.1920034

cis-trans-cis-[Pt(N3)2(OH)2(NH3)2]

Pt	0.1309946	0.0499285	-0.0618477
N	2.2600038	0.1787494	-0.1739474
N	-0.2472912	2.1229016	0.1435681
N	-1.9244455	-0.0309246	-0.0205494
N	0.2583833	-2.0046942	-0.2063286
O	0.1313132	0.1911194	1.9799547
O	0.3827542	0.1802992	-2.0947382
H	-0.6864343	-0.2623299	2.2830759
H	0.1234377	-0.6929792	-2.4647330

H	-1.2281342	2.2422515	-0.1591505
H	-0.1936098	2.2177816	1.1773241
H	2.7246469	-0.6581163	0.2154992
H	2.3510508	0.1949315	-1.2111081
H	2.6907481	1.0122789	0.2488932
H	0.3572449	2.7969237	-0.3456257
N	-2.4533685	-0.8538672	-0.7646825
N	1.2249442	-2.5133243	0.3438569
N	-3.0470311	-1.5934482	-1.4239689
N	2.1285928	-3.0654815	0.8213078

REFERENCES

- ¹M. J. G. Peach, P. Benfield, T. Helgaker, and D. J. Tozer, *The Journal of Chemical Physics* **128**, 044118 (2008).
- ²J. M. H. Olsen, S. Reine, O. Vahtras, E. Kjellgren, P. Reinholdt, K. O. Hjorth Dundas, X. Li, J. Cukras, M. Ringholm, E. D. Hedegård, R. Di Remigio, N. H. List, R. Faber, B. N. Cabral Tenorio, R. Bast, T. B. Pedersen, Z. Rinkevicius, S. P. A. Sauer, K. V. Mikkelsen, J. Kongsted, S. Coriani, K. Ruud, T. Helgaker, H. J. A. Jensen, and P. Norman, *The Journal of Chemical Physics* **152**, 214115 (2020), <https://doi.org/10.1063/1.5144298>.